pubs.acs.org/Biomac

Article

Investigation of N-Substituted Morpholine Structures in an Amphiphilic PDMS-Based Antifouling and Fouling-Release Coating

Amanda K. Leonardi, Riddhiman Medhi, Aria Zhang, Nilay Düzen, John A. Finlay, Jessica L. Clarke, Anthony S. Clare, and Christopher K. Ober*

Cite This: https://doi.org/10.1021/acs.biomac.1c01474

Read Online

ACCESS | Metrics & More | Article Recommendations | Supporting Information

ABSTRACT: Biofouling is a major disruptive process affecting the fuel efficiency and durability of maritime vessel coatings. Previous research has shown that amphiphilic coatings consisting of a siloxane backbone functionalized with hydrophilic moieties are effective marine antifouling and fouling-release materials. Poly(ethylene glycol) (PEG) has been the primary hydrophilic component used in such systems. Recently, the morpholine group has emerged as a promising compact alternative in antifouling membranes but is yet to be studied against marine foulants. In this work, the use of morpholine moieties to generate amphiphilicity in a poly(dimethylsiloxane) (PDMS)-based antifouling and fouling-release coating was explored. Two separate coating sets were investigated. The first set examined the incorporation of an N-substituted morpholine amine, and while these coatings showed promising fouling-release properties for *Ulva linza*, they had unusually high settlement of spores compared to controls. Based on those results, a second set of materials was synthesized using an N-substituted morpholine amide to probe the source of the high settlement and was found to significantly improve antifouling performance. Both coating sets included PEG controls with varying lengths to compare the viability of the morpholine structures as alternative hydrophilic groups. Surfaces were evaluated through a combination of bubble contact angle goniometry, profilometry, X-ray photoelectron spectroscopy (XPS), and marine bioassays against two soft fouling species, *U. linza* and *Navicula incerta*, known to have different adhesion characteristics.

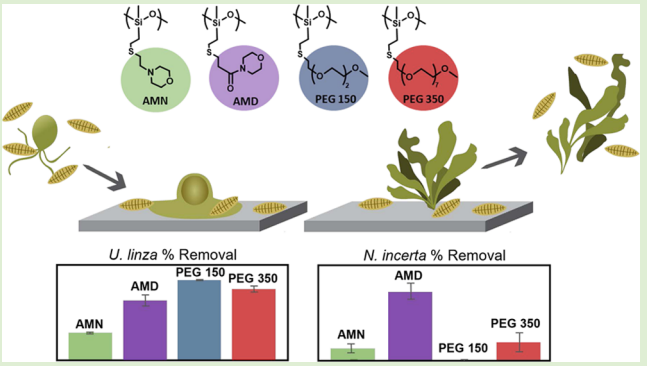

INTRODUCTION

Marine biofouling has surprisingly large and far-reaching effects on naval and civilian maritime industries, and even minimal levels of fouling can severely impact operations. Studies have indicated that a heavy slime layer on a mid-sized naval ship can lead to a 20% increase in resistance at a typical cruising speed due to increased drag[1] and can increase fuel consumption by 10.3%, resulting in a $1.2 million increase in fuel costs per ship per year.[2] Instrument function is also at risk, with recorded transmission losses in the sonar performance of up to 9.09 dB.[3] Over the years, the main control of fouling has been through the use of biocidal coatings. By the second half of the 20th century, biocidal coatings had improved considerably, and extremely effective mechanisms to prevent fouling on ships' hulls had been identified.[4,5] Unfortunately, many of the biocides employed were found to accumulate in marine environments, adversely affecting nontarget organisms.[6−10] Over the past 20−30 years, the development of nonbiocidal antifouling and fouling-release coatings has garnered greater attention, and a few key materials have been recognized as performing well in those domains.

Successful nonbiocidal coatings designed to prevent settlement of marine organisms often rely on hydrophilic surfaces that create a hydration layer to act as a physical and energetic barrier to the adsorption of biomolecules.[11] A more simplistic view of this is that a tightly bound hydration layer inhibits the initial deposition of marine adhesives, which are largely hydrophobic.[12] Fouling-release surfaces are composed of low surface energy materials with soft mechanical properties, designed to limit the adhesive interactions between the organism and surface to facilitate easy removal. Poly(dimethylsiloxane) (PDMS) is particularly well suited to promote the removal of biofouling, but it is an extremely poor antifouling material in aqueous environments as proteins and organisms readily adsorb to its surface. To generate surfaces that perform as both antifouling and fouling-release surfaces,

Received: November 29, 2021
Revised: March 30, 2022

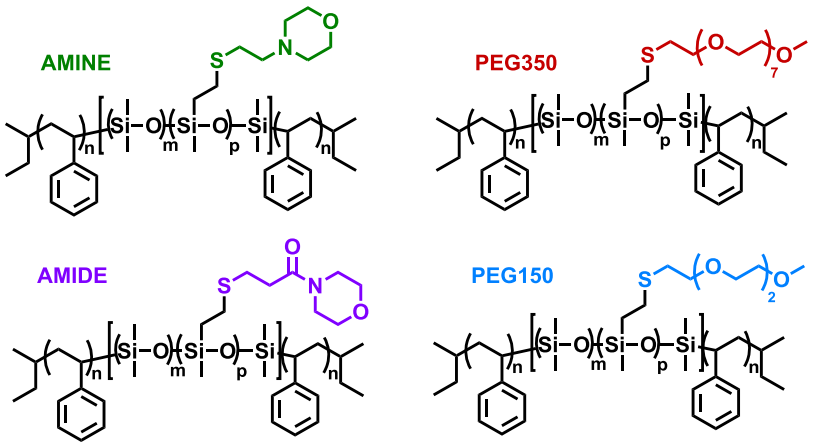

Figure 1. Functionalized polymer structures used in morpholine coatings. Amine and 350 g/mol PEG-functionalized backbones (above) were used in the first coating set, while all four were included in the second. Triblocks are shown, but all coatings were a 50/50 blend of triblock and diblock.

siloxane materials have been modified with hydrophilic components to produce amphiphilic surfaces. Poly(ethylene glycol) (PEG) has proved invaluable in the construction of antifouling surfaces, owing largely to its uncharged hydrogen bond acceptor groups, and has been used extensively in both marine and biomedical applications. In combination with siloxanes, it has produced many successful amphiphilic marine antifouling and fouling-release surfaces.[13−20]

While PEG has been considered the gold standard in laboratory-scale experimental coatings, indications of possible immunogenicity in humans and concerns related to its long-term chemical stability in marine environments have increased the scrutiny of its widespread use and have precipitated the exploration of alternatives.[21−24] Several hydrophilic alternatives are possible, but the majority have severe shortcomings for antifouling applications. For example, while cationic quaternary ammonium groups are hydrophilic and have antimicrobial properties, they have shown severe fouling by marine organisms.[25−27] Similarly, carboxylic acid or hydroxy groups are hydrophilic but can interact with adhesives and promote attachment of a range of marine species.[28,29] (An exception to the poor behavior of charged groups is zwitterion units, which are charge neutral and have shown success in antifouling coatings.[25,27,30−35]) Morpholine, an uncharged, six-membered heterocycle, with both an amine (AMN) and ether functionality, is a compact moiety and easily incorporated in a number of structures as a potential PEG replacement.

Morpholine has long been used to increase the aqueous solubility of drug molecules,[36−39] and more recently, it has shown promise in generating a hydrophilic character on surfaces and coatings used in biomedical and membrane antifouling applications. Amphiphilic copolymers of poly(vinylidene fluoride) (PVDF) and poly(2-*N*-morpholino)ethyl methacrylate (PMEMA) were used as additives in the construction of PVDF ultrafiltration membranes and led to an over 80% decrease in bovine serum albumin (BSA) adsorption and imparted control over pore size and membrane permeability.[40] Elsewhere, PMEMA was used in a switchable polymer brush coating for protecting key functional groups from organic fouling.[41] Micropatterned substrates composed of poly(*N*-acryloylmorpholine) (PAcMo) and poly(*N*-isopropylacrylamide) (PNIPAM) were developed to grow aligned cell sheets, in which cell growth was inhibited on PAcMo and only grew in an aligned manner on PNIPAM domains.[42] Researchers have also grafted PAcMo to electrospun fibers to generate low fouling materials that could be employed as implantable scaffolds able to resist nonspecific protein absorption and cell binding.[43,44] PAcMo has also been used to modify PVDF membranes to improve protein resistance and hemocompatibility, in one study demonstrating a flux recovery ratio of 98.4% when filtering BSA solutions.[45−48] While effective protein and cell binding resistance using morpholine-based materials has been demonstrated in other fields, its combination with PDMS for marine antifouling and fouling release has not yet been investigated.

In this study, the incorporation of morpholine onto a polystyrene-*b*-poly(dimethylsiloxane-*r*-vinylmethylsiloxane) (PS-PDMS) block copolymer system was investigated (Figure 1). Using N-substituted morpholine structures, differences in performance were probed to assess their viability for use in antifouling and fouling-release coatings. Two coating sets were tested, the first investigating a series of coatings functionalized with an N-substituted morpholine amine, which showed promising fouling-release performance, but unusually a high settlement of *Ulva linza* spores. Building from these results, a second coating set examined an N-substituted morpholine amide (AMD) and found better broad-spectrum performance using this structure. Both coating sets were evaluated in marine assays against two species of fouling algae, *U. linza* and *Navicula incerta*, and the results were correlated to their surface properties.[49]

EXPERIMENTAL SECTION

Materials. All chemicals were purchased from Sigma-Aldrich, and solvents were obtained from VWR and used as received unless specified otherwise. Hexamethylcyclotrisiloxane (D3) and 1,3,5-trivinyl-1,3,5-trimethylcyclotrisiloxane (V3) were purchased from Gelest, Inc. Anhydrous ethanol was purchased from Fisher Scientific. Benzene was stirred over *n*-butyl lithium and diphenylethylene, distilled, and freeze−pump−thawed to degas. Styrene was dried over calcium hydride, distilled, and freeze−pump−thawed to degas. D3 was dissolved in benzene and stirred over calcium hydride for 24 h at which point a living anionic styrene polymerization was added and allowed to stir until the orange color had completely disappeared. The benzene was subsequently distilled, and the D3 was sublimed, and then the solution was freeze−pump−thawed to degas. Solution concentration was determined using nuclear magnetic resonance spectroscopy (NMR). Tetrahydrofuran (THF) was stirred over calcium hydride and distilled into a flask containing sodium and benzophenone and allowed to stir for several days, at which point it

https://doi.org/10.1021/acs.biomac.1c01474
Biomacromolecules XXXX, XXX, XXX−XXX

was distilled and freeze−pump−thawed to degas. V3 was stirred over calcium hydride, distilled, and freeze−pump−thawed to degas. Tosyl chloride was dissolved with ether and washed with 1 M NaOH and then crystallized by cooling. Glass slides were purchased from Fisher Scientific. Polystyrene-*block*-poly(ethylene-*ran*-butylene)-*block*-polystyrene (SEBS) and polystyrene-*block*-poly(ethylene-*ran*-butylene)-*block*-polystyrene-*graft*-maleic anhydride (MA-SEBS) were generously provided by Kraton, Inc. Zoospores were obtained from mature plants of *U. linza* by the standard method.[49] Cells of *N. incerta* were cultured in F/2 medium.

Synthesis. *PS-P(DMS/VMS) Backbone Synthesis.* PS-P(DMS/VMS) backbones were prepared according to a previously reported method[27] (see Scheme 1). In brief, in a glovebox, *sec*-butyl lithium

Scheme 1. Synthesis of Diblock and Triblock PS-P(DMS/VMS) Polymer Backbone and Functionalization via Thiol−Ene Click Reaction

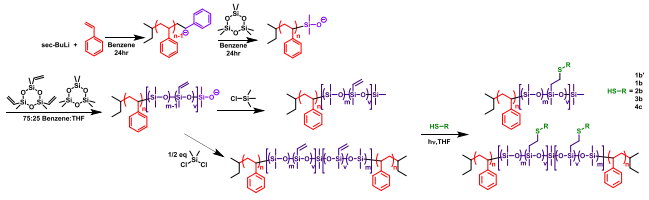

was added to a flask charged with benzene and a stir bar, followed by the dropwise addition of styrene, leading to the development of a deep orange color. The reaction progressed overnight before sampling, followed by the addition of a solution of D3 in benzene. After the complete disappearance of the orange color, indicative of the live styrene anion, THF was added and the reaction was allowed to continue for 2 h. At this point, the addition of a solution of V3 in THF by a syringe pump had begun and allowed to progress over 48 h. After addition, the polymerization was reacted for an additional 24 h. The polymerization was then split, one half being end-capped with chlorotrimethylsilane for the formation of diblock and the other half coupled using a solution of dichlorodimethylsilane in THF. Coupling was done by adding 75% of the coupling agent directly, followed by the addition of the remaining 25% of the coupling agent by a syringe pump over a 24 h period. Polymers were precipitated directly into a 4/1 (v/v) mixture of methanol and deionized water and allowed to stir overnight. Polymers were collected by vacuum filtration and dried overnight in a vacuum oven at 55 °C.

*PEG-Mesylate (**1a′**).* Poly(ethylene glycol) monomethyl ether (M_n = 350 g/mol) (20.0 g, 57.1 mmol) and *N*,*N*-diisopropylethylamine (DIPEA, 11 mL, 63.1 mmol) were dissolved in tetrahydrofuran under an inert atmosphere. The solution was cooled to 0 °C, and mesyl chloride (4.8 mL, 62.0 mmol) was added dropwise. The reaction was warmed to room temperature and left to react for 12 h, during which a precipitate formed. The precipitate was filtered off, and the reaction mixture was passed through a silica plug. The solution was concentrated under reduced pressure to yield a brown oil. Yield: 72.0%. Proton NMR (400 MHz, $CDCl_3$): δ (ppm)—4.36 (t, 2H), 3.74 (t, 24H), 3.64 (m, 2H), 3.53 (m, 2H), 3.32 (s, 3H), 3.02 (s, 3H).

*PEG-Thiol (**1b′**).* **1a′** (15 g, 29.7 mmol) and thiourea (2.3 g, 29.7 mmol) were dissolved in ethanol. The solution was refluxed under an inert atmosphere for 3 h. NaOH (1.4 g, 35.5 mmol) dissolved in a minimal amount of deionized water was added and refluxed for a further 2 h. The reaction was cooled to room temperature and concentrated under reduced pressure. The residue was diluted with deionized water, neutralized with HCl, and then extracted three times with dichloromethane (DCM). The organic layer washings were combined, dried over Na_2SO_4, and concentrated under reduced pressure to yield a light-yellow oil. The product was used without further purification. Yield: 40.0%. Proton NMR (400 MHz, $CDCl_3$): δ (ppm)—3.70 (m, 2H), 3.57−3.67 ppm (m, 24H), 3.53 (m, 2H), 3.36 (s, 3H), 2.68 (q, 2H), 1.58 (t, 1H).

Different procedures were used for the PEG-thiol generation in the production of two different coating sets. After the first coating set, the optimization of the reaction conditions was carried out and used for the second set.

*350 PEG-Tosylate (**1a**).* Poly(ethylene glycol) monomethyl ether (M_n = 350 g/mol) (3.83 g, 10.9 mmol) was dissolved in dichloromethane with triethylamine (3.36 mL, 24.1 mmol). The solution was cooled to 0 °C, and purified tosyl chloride (2.30 g, 12.6 mmol) was added by the spatula full. The reaction was warmed to room temperature and left to react for 12 h. The reaction mixture was successively washed with 1 M HCl, sat. $NaHCO_3$, and distilled water until washings were at neutral pH. The organic layer was dried over Na_2SO_4 and concentrated under reduced pressure. The resulting residue was purified by column chromatography using an eluent mixture of 60/40 DCM/hexanes to 90/10 DCM/MeOH. Yield: 72%. Proton NMR (400 MHz, $CDCl_3$): δ (ppm)—7.78 ppm (d, 2H), 7.32 (d, 2H), 4.14 (t, 2H), 3.66 (t, 2H), 3.62 (m, 24H), 3.53 (m, 2H), 3.36 (s, 3H), 2.43 (s, 3H).

*350 PEG-Thiol (**1b**).* **1a** (4.38 g, 8.65 mmol) and thiourea (0.79 g, 10.4 mmol) were dissolved in a 2:1 mixture of ethanol and deionized water. The solution was refluxed under an inert atmosphere for 3 h. NaOH (0.52 g, 13.0 mmol) dissolved in a minimal amount of deionized water was added, and the reaction was refluxed for a further 2 h. The reaction mixture was cooled to room temperature and concentrated under reduced pressure. The residue was diluted with deionized water and neutralized with 1 M HCl and then extracted three times with DCM. The organic layer washings were combined, dried over Na_2SO_4, and concentrated under reduced pressure to yield a light-yellow oil. The product was used without further purification. Yield: 86.4%. Proton NMR (400 MHz, $CDCl_3$): δ (ppm)—3.57−3.71 ppm (m, 26H), 3.52 (m, 2H), 3.35 (s, 3H), 2.70 (m, 2H), 1.57 (t, 1H).

*150 PEG-Tosylate (**2a**).* An identical procedure to **1a** was employed using poly(ethylene glycol) monomethyl ether (M_n = 150 g/mol) (0.89 g, 5.93 mmol), tosyl chloride (1.55 g, 8.13 mmol), and triethylamine (0.87 mL, 10.8 mmol). Yield: 87.3%. Proton NMR (400 MHz, $CDCl_3$): δ (ppm)—7.79 (d, 2H), 7.33 (d, 2H), 4.15 (t, 2H), 3.67 (t, 2H), 3.57 (m, 6H), 3.52 (m, 2H), 3.36 (s, 3H), 2.44 (s, 3H).

*150 PEG-Thiol (**2b**).* An identical procedure to **1b** was employed using **2a** (1.65 g, 5.39 mmol), thiourea (0.47 g, 6.17 mmol), and NaOH (0.31 g, 7.75 mmol). Yield: 83.7%. Proton NMR (400 MHz, $CDCl_3$): δ (ppm)—3.64 (m, 8H), 3.54 (m, 2H), 3.37 (s, 3H), 2.69 (m, 2H), 1.58 (t, 1H).

*N-(2-Chloroethyl)morpholine (**3a**).* 2-Chloroethylmorpholine hydrochloride (6.23 g, 33.5 mmol) was dissolved in deionized water and cooled to 0 °C. A solution of NaOH (2.95 g, 73.8 mmol) in deionized water was added dropwise and allowed to stir at room temperature for 1 h. The solution was extracted three times with ethyl acetate, and then the organic layer was dried over Na_2SO_4. The solvent was removed under reduced pressure. Yield: 81.4%. Proton NMR (400 MHz, $CDCl_3$): δ (ppm)—3.69 (m, 4H), 3.56 (t, 2H), 2.70 (t, 2H), 2.49 (m, 4H).

*N-(2-Mercaptoethyl)morpholine (**3b**).* **3a** (2.03 g, 13.6 mmol), thiourea (1.54 g, 20.2 mmol), and KI (1.12 g, 6.72 mmol) were dissolved in a 95% mixture of ethanol and deionized water. The solution was refluxed under an inert atmosphere for 3 h. NaOH (0.81 g, 20.3 mmol) dissolved in a minimal amount of deionized water was added, and the solution was refluxed for a further 2 h. The reaction mixture was cooled to room temperature and concentrated under reduced pressure. The residue was neutralized with 1 M HCl and then extracted three times with DCM. The organic layer was dried over Na_2SO_4 and concentrated under reduced pressure to yield a yellow oil. The product was used without further purification. Yield: 82.8%. Proton NMR (400 MHz, $CDCl_3$): δ (ppm)—3.71 (m, 4H), 2.59 (m, 4H), 2.45 (m, 4H), 1.23 (t, 1H).

*3-(Tritylthio)propionic Acid (**4a**).* 3-Mercaptopropionic acid (5 g, 47.1 mmol) was dissolved in 50 mL dichloromethane. Trityl chloride (13.1 g, 47.1 mmol) was separately dissolved in 30 mL DCM and added dropwise to the solution of 3-mercaptopropionic acid using an addition funnel. The reaction proceeded overnight. A solid white

https://doi.org/10.1021/acs.biomac.1c01474
Biomacromolecules XXXX, XXX, XXX−XXX

precipitate formed, which was collected by vacuum filtration while rinsing with cold diethyl ether. Yield: 83.7%. Proton NMR (400 MHz, $(CD_3)_2SO$): δ (ppm)—12.24 (s, 1H) 7.33 (m, 12H), 7.25 (m, 3H), 2.27 (m, 2H), 2.16 (m, 2H).

*3-(Tritylthio)-1-(4-morpholinyl)-1-propanone (**4b**).* 1-Ethyl-3-(3-dimethylaminopropyl)carbodiimide (EDC) (7.60 g, 39.6 mmol) was dissolved in 200 mL of a 50/50 DCM/DMF mixture, allowing 30−40 min to fully dissolve. The solution was cooled to 0 °C, at which point ethyl cyano(hydroxyimino)acetate (5.60 g, 39.4 mmol) and **4a** (13.74 g, 39.4 mmol) were directly added, causing the solution to take on a yellow-orange color. Morpholine (3.40 mL, 38.6 mmol) and DIPEA (6.87 mL, 71.6 mmol) were subsequently added to the reaction. The reaction proceeded for 16 h under an inert atmosphere. The solvent was removed under reduced pressure, and the residue was redissolved in chloroform and extracted three times each with 1 M HCl, sat. Na_2CO_3, and sat. NaCl. The organic layer was dried over Na_2SO_4, and the solvent was removed under reduced pressure. The resulting solid was recrystallized in ethanol to yield a pale-yellow solid. Yield: 58.3%. Proton NMR (400 MHz, $CDCl_3$): δ (ppm)—7.44 (d, 6H), 7.28 (t, 6H), 7.20 (t, 3H), 3.60 (t, 2H), 3.53 (q, 4H), 3.16 (t, 2H), 2.56 (t, 2H), 2.10 (t, 2H).

*(3-Mercapto)-1-(4-morpholinyl)-1-propanone (**4c**).* **4b** (9.59 g, 23.0 mmol) was dissolved in 40 mL DCM and cooled to 0 °C. Triethylsilane (4 mL, 47.2 mmol) was added to the solution, followed by the dropwise addition of trifluoroacetic acid (20 mL) at which point a light-yellow color developed. The reaction was stirred for 1.5 h at 0 °C and then for 30 min at room temperature. The solvent was removed under reduced pressure. The residue was filtered using cold methanol to remove solids, and the methanol was subsequently removed under reduced pressure. The residue was dissolved in DCM and washed three times each with sat. $NaHCO_3$ and sat. NaCl. The organic layer was dried over Na_2SO_4, and the solvent was removed under reduced pressure. The product separated into two layers, and the bottom product layer was collected using a separatory funnel. Residual amounts of triethylsilane were still present in the sample but were found not to interfere with the click reaction, so the product was used without further purification. Yield: 51.6%. Proton NMR (400 MHz, $CDCl_3$): δ (ppm)—3.66 (m, 6H), 3.46 (m, 2H), 2.82 (q, 2H), 2.64 (t, 2H), 1.75 (t, 1H).

Thiol−Ene Click Reactions. In a typical reaction, polymer and 2,2-dimethoxy-2-phenylacetophenone (DMPA, 0.2 mol, with respect to polymer vinyl groups) were dissolved in DCM, to which **1b′**, **1b**, **2b**, **3b**, or **4c** (5 mol, with respect to polymer vinyl groups) was added. For example, in the preparation of the amide-functionalized diblock polymer for coating AMD-3.9, 0.75 g of unfunctionalized polymer was dissolved in approx. 10 mL of DCM with 12 mg of DMPA. To this was added 0.213 g of **4c**. The solution was degassed by bubbling with nitrogen for 15 min, and then the reaction vessel was exposed to 365 nm UV for 2−6 h. The polymer was precipitated into methanol, collected by filtration, and then reprecipitated two more times from THF into a 4/1 methanol/water mixture and collected by vacuum filtration. For samples with higher functionalization, precipitated mixtures were centrifuged to collect polymer more easily. Samples were dried under vacuum at 55 °C overnight.

Coating Preparation. Coatings were prepared according to a previously reported method.[55] In brief, samples were prepared on glass microscope slides, which were freshly cleaned in a piranha solution of 70/30 concentrated sulfuric acid and 30% hydrogen peroxide. Note: piranha solution is a strong oxidizer and should be handled with caution. Slides were then thoroughly rinsed with deionized water, dried, and immersed in 2 vol % of 3-aminopropyltriethoxysilane (APTES) in anhydrous ethanol solution overnight. Slides were rinsed extensively with water and ethanol and then annealed for 4 h under vacuum at 120 °C. A 7 wt % solution of maleic anhydride-SEBS in toluene was spun-coat (2000 rpm, 30 s) and annealed for 12 h at 120 °C under vacuum. Lastly, three layers of a 12 wt % solution of SEBS in toluene were successively spun-cast (2000 rpm, 30 s), followed by a 12 h anneal under vacuum at 120 °C. Functionalized block copolymers were spray-coated using a Badger model 250 airbrush onto the SEBS tie layer at 50 psi from a 10 mg/mL solution in 19/1 DCM/toluene for the first set and 19/1 DCM/dodecane for the second set. Surfaces were annealed for 12 h at 60 °C under vacuum and then for 12 h at 120 °C.

Fouling Assays. *U. linza.* All coatings were equilibrated in artificial seawater (ASW) (Tropic Marin) for 72 h prior to testing. Assays were carried out at room temperature (ca. 20 °C). A suspension of zoospores (approx. 1.0×10^6 spores/mL) was added to individual compartments of quadriPERM dishes containing three replicate slides. After 45 min, the slides were gently washed to remove unsettled spores. The attached spores were fixed using 2.5% glutaraldehyde in ASW. The density of zoospores attached to the surface was counted using an image analysis system attached to a fluorescence microscope (Zeiss Axioskop 2). Spores were visualized by autofluorescence of chlorophyll. Counts were made for 30 fields of view (each 0.15 mm^2) on each slide.

For removal experiments, spores were settled on six replicate slides for 45 min and then washed as described above. Spores were cultured using supplemented seawater medium for 7 days to produce sporelings.[50] Sporeling growth medium was refreshed every 48 h. Sporeling biomass was determined by chlorophyll fluorescence in a Tecan (Spark 20M) fluorescence plate reader. Biomass was quantified in terms of relative fluorescence units (RFUs), which was calculated from the mean of 70-point fluorescence readings. Removal of sporelings from amine coatings was assessed using an impact pressure of 55 kPa from a water jet sprayed across the central area of each slide, while the removal of sporelings from amide coatings was assessed using a shear stress of 42 Pa in a turbulent flow cell.[51,52] The different methods used reflect the adhesion strengths of the sporelings to the surfaces. The relatively weak adhesion on the morpholine amide coatings required assessment using the more sensitive water channel rather than the water jet used for the morpholine amine coatings. Biomass remaining was determined using the fluorescence plate reader (as described above). The percentage removal was calculated from readings taken before and after exposure to the shear stress.

N. incerta. All coatings were equilibrated in ASW for 72 h prior to testing. Assays were carried out at room temperature (ca. 20 °C). Suspensions of *N. incerta* cells (approx. 1.5×10^5 cells/mL) in ASW settled on three replicate slides of each sample in individual quadriPERM dishes. The diatoms were settled for 2 h, before shaking for 5 min on an orbital shaker at 60 rpm, and then gently washed in ASW to remove unattached cells. The 2 h settlement period allowed time for the diatom cells to contact the surface and initiate attachment processes. Samples were fixed in 2.5% glutaraldehyde, air-dried, and the density of the attached cells was counted using an image analysis system attached to a fluorescence microscope. Cells were visualized by autofluorescence of chlorophyll. Counts were made for 15 fields of view (each 0.15 mm^2) per slide for the amine coating set and 30 fields of view (each 0.15 mm^2) per slide for the amide coating set.

A further three replicates were settled with cells as described above. Slides with attached cells were exposed to a shear stress of 40 Pa for the amine coating set and 32 Pa for the amide coating set in a water channel for 5 min. Samples were fixed, and the number of cells remaining attached was counted as described above. Results were expressed as percent removal, derived from the difference between the initial attachment density and final density after exposure to the shear stress.

RESULTS AND DISCUSSION

Morpholine Amine Coating Set. *Material Synthesis and Coating Preparation.* Preparation of polystyrene-*b*-poly(dimethylsiloxane-*r*-vinylmethylsiloxane) (PS-PDMS) backbones followed a previously reported procedure.[53−58] Pendant vinyl groups along the PDMS block facilitate simple backbone modification to modulate chemistry and behavior at the coating surface. A blend of diblock and triblock was used, since previously, a mixture of the two architectures functionalized with PEG showed a higher removal of *U. linza* than the triblock copolymer alone.[54] Polymers were designed with short

https://doi.org/10.1021/acs.biomac.1c01474
Biomacromolecules XXXX, XXX, XXX−XXX

Table 1. Polymer Functionalization and Corresponding Sample Codes for PS-PDMS Morpholine Amine Coatings

code	side group	backbone structure	mol % vinyl[a]	mol %[a]	wt %[b]	coating mol %[c]	coating wt %[c]
M1.2	morpholine amine	triblock	3.28	0.95	1.99	1.20	1.6
		diblock	3.27	1.45	1.30		
M2.9	morpholine amine	triblock	5.49	2.66	3.72	2.87	4.0
		diblock	5.53	3.08	4.30		
M3.6	morpholine amine	triblock	10.70	2.75	3.76	3.56	4.8
		diblock	9.62	4.38	5.86		
P1.2	PEG M_n = 350	triblock	3.28	1.35	4.37	1.20	3.9
		diblock	3.27	1.05	3.48		
P2.6	PEG M_n = 350	triblock	5.49	2.59	8.60	2.61	8.7
		diblock	5.53	2.63	8.73		

[a]Mole percent functionalized monomer units with respect to PDMS block calculated using ^{1}H NMR. [b]Weight percent functional group with respect to the total polymer molecular weight. [c]Coatings consist of a 50/50 mixture diblock and triblock. Coating content calculated by averaging diblock and triblock values.

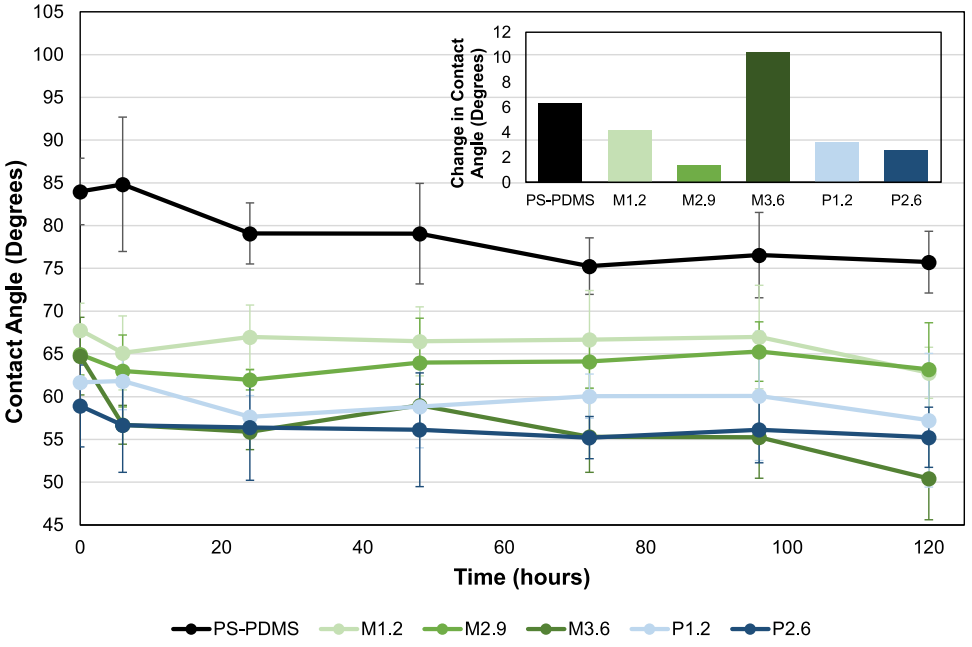

Figure 2. Captive bubble contact angles over a 4 day period on PS-PDMS morpholine amine coatings. The inset indicates the total change in contact angle from the initial value for each coating. All coatings showed a drop in contact angle, with M3.6 showing the most drastic change, occurring mainly in the first 12 h. Error bars are standard deviations.

PS blocks (6−8k) and long PDMS blocks (25−35k); diblocks were coupled to generate triblocks, resulting in PDMS blocks of 50−70k with two terminal PS blocks of equal length. Gel permeation chromatography (GPC) chromatograms and molar masses of the polymer backbones are listed in Figure S1 and Table S1.

Modification of the backbone was done using a thiol−ene click reaction to pendant vinyl groups on the PDMS block. A thiol was introduced on the corresponding morpholine or PEG structures and attached at different loading percentages, as detailed in Table 1, calculated based on NMR spectra presented in Figure S2. Corresponding sample codes, which are based on the mole percent loading of the hydrophilic group, are also included. Notably, backbone modification resulted in low attachment percentages at or below 50%. It has been reported elsewhere that thiol−ene reactions exhibit retarded kinetics and diminished efficiency in the presence of amines, which is especially pronounced on vinyl siloxane substrates.[59−61] This is a result of the deprotonation of the thiol by the amine to the thiolate anion, which reacts with a thiyl radical to form a two-sulfur-three-electron-bonded disulfide species. This constraint, coupled with the limited access of the small hydrophilic molecule to vinyl groups buried within the large hydrophobic PDMS backbone (which has been observed previously),[56] likely explains why the functionalization efficiencies were so low.

Coatings were assembled using a layered structure, which has been reported extensively elsewhere,[55,62,63] employing a tie layer of commercially available thermoplastic elastomer, polystyrene-*b*-poly(ethylene-*r*-butylene)-*b*-polystyrene (SEBS). The tie layer serves a dual purpose: to aid in the stable attachment of the PS-PDMS to the surface and to provide the necessary mechanical properties to optimize fouling release. Substrates are functionalized with an amino silane, onto which a maleic anhydride-functionalized SEBS is deposited. The amino groups react with the maleic anhydride to covalently tether the polymer to the surface. On top of this, a thick layer (∼1 mm) of unfunctionalized SEBS is built up through successive spin coating. This SEBS was previously reported to have Young's modulus of 1.2 MPa,[55] which is within the

https://doi.org/10.1021/acs.biomac.1c01474
Biomacromolecules XXXX, XXX, XXX−XXX

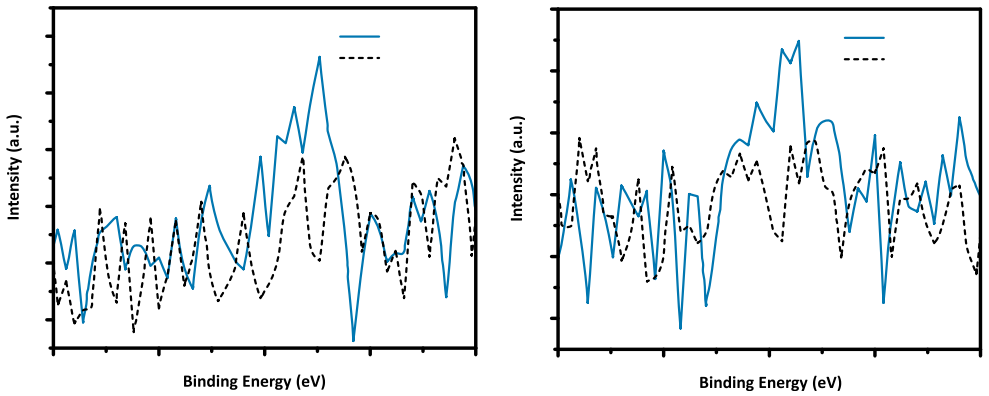

Figure 3. High-sensitivity XPS scans for N 1s in M1.2 (left) and M3.6 (right) surfaces. Coatings show no nitrogen signal in the dry state (dashed line), but after 72 h immersion in water, a small but detectable peak is seen, confirming the presence of nitrogen at the surface (solid line).

optimal range for the promotion of fouling release. The thick layer is used because an increase in film thickness has been shown to correlate with a decrease in biofoulant adhesion strength.[64−66] The functionalized PS-PDMS is spray-coated on top of the SEBS to mimic typical application conditions used on a boat hull. The PS end groups in the PS-PDMS are designed to interact with the PS domains in the underlayer to physically cross-link it to the surface. Also included in the marine testing were two control surfaces: a clean glass slide as a hydrophilic reference and a standard cross-linked PDMS elastomer (PDMSe) as a hydrophobic control. Surface roughness values, as well as the maximum feature height of coatings, are detailed in Table S2. All surfaces show relatively high roughness values and feature sizes, which can be attributed to the use of spray coating deposition methods.

Surface Characterization. Bubble contact angle measurements were done to assess changes in surface wettability with backbone modification. The captive bubble technique immerses the sample in a liquid and uses a bubble of air instead of a liquid droplet to measure the contact angle at the surface. This allows for wettability to be measured under conditions that imitate the coating operating environment more directly.[67] Contact angle changes were measured over a 4 day period as the coatings were submerged in water. Values were corrected for surface roughness, using the Wenzel relation and roughness ratios detailed in Table S2. Notably, the initial captive bubble contact angles (at 0 h) taken immediately after immersion closely resemble static contact angle data. Initial captive bubble contact angle data, in Figure 2, shows that functionalization with both morpholine and PEG imparts significant hydrophilicity to the surfaces, lowering the measured contact angle compared to the unfunctionalized control. All morpholine coatings possessed very similar initial contact angle values around 65°. While M1.1 and M2.9 contact angles remained relatively constant over the measurement period, M3.6 showed a more significant decrease over time, with an almost 15° drop in contact angle. Coatings P1.2 and P2.6 had lower initial contact angles than the morpholine coatings (62 and 59°, respectively), but like coatings M1.2 and M2.9 showed little change in contact angle over time. Coating M3.6 had the lowest final contact angle among all of the coatings, even marginally lower than the PEG coatings. It is also notable that although M3.6 and P2.6 have similar mole percent of the hydrophilic group, P2.6 has a much higher weight percent because of the length of the PEG (4.8 and 8.7 wt % for M3.6 and P2.6, respectively). This would indicate that the compact morpholine structure hydrates the surface more efficiently than PEG.

Surface analysis was done to probe the chemical composition of coating surfaces. X-ray photoelectron spectroscopy (XPS) survey scans show that the elemental compositions of the surfaces are very similar to that of unfunctionalized PS-PDMS (Table S3). All coatings show significantly less carbon at the surface than would be theoretically expected. This result aligns with the fact that PDMS has a much lower surface energy than PS, 21.9 versus 38.3 mN/m, respectively.[68] The PDMS block thus makes up the bulk of the surface, burying the polystyrene block. Higher functionalization, with either morpholine or PEG, generally led to higher carbon content and greater deviation from the composition of the unfunctionalized PS-PDMS control. This would indicate that the surface is enriched with the small-molecule side groups.

X-ray photoelectron spectroscopy (XPS) scans of the N 1s region of the morpholine coatings, both before and after immersion in water, give greater insight into the behavior of the side groups (Figure 3). In the dry state, there is no evidence of nitrogen as the peak intensity in the N 1s region is negligible compared to that of the baseline. However, after exposure to water for 72 h, a very small but detectable peak can be seen in the N 1s region confirming the presence of nitrogen at the surface. This would indicate that the surface coating is undergoing a rearrangement upon exposure to water, with morpholine side groups coming to the surface. Despite showing no nitrogen at the surface in the dry state, the initial contact angles of all of the morpholine coatings are lower than that of the unfunctionalized PS-PDMS. It is likely that morpholine is at the surface in the as-deposited state, but the percent of nitrogen lies below the detection limit of the instrument (usually reported to be 0.1−1 atom %).[69] This indicates that only a relatively small amount of hydrophilic group is necessary to achieve a dramatic effect on surface behavior.

Fouling Assays. *N. incerta* diatoms are a unicellular species of algae that form biofilms or slimes on surfaces. They are not motile in the water column and settle through gravity, relying on water movement to transport them to surfaces.[70] Once settled, they excrete extracellular polymeric substances that act as both an adhesive and a motility polymer that facilitates movement across surfaces.[71,72] In previous studies, *N. incerta* has exhibited high settlement and strong adhesion to PDMS surfaces and is less likely to settle and is more easily removed from hydrophilic surfaces.[73] In initial attachment studies

https://doi.org/10.1021/acs.biomac.1c01474
Biomacromolecules XXXX, XXX, XXX−XXX

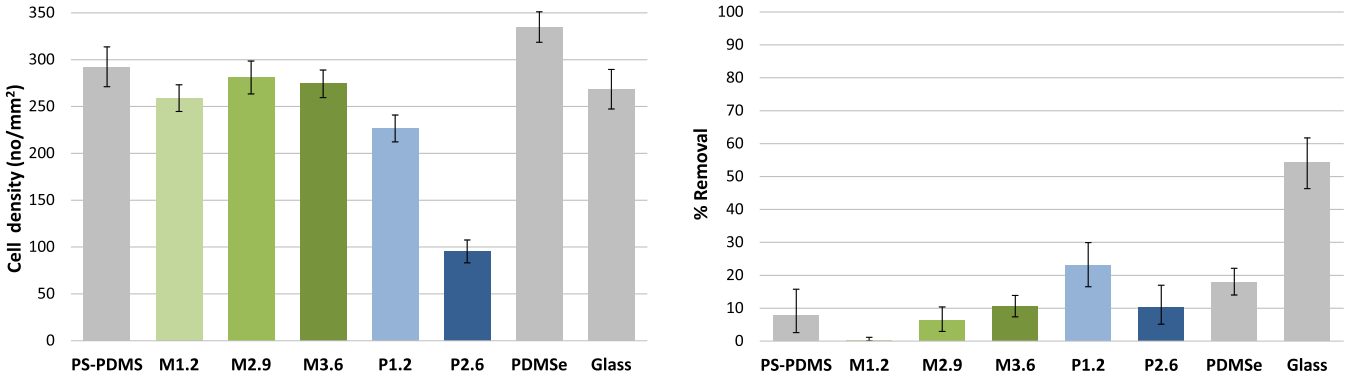

Figure 4. Density of attached *N. incerta* cells after initial settlement on PS-PDMS morpholine amine coatings (left) and percent of removed cells after exposure to a shear stress of 40 Pa (right). Each point is the mean from 45 counts on three replicate slides. Bars show 95% confidence limits for settlement and 95% confidence limits derived from arcsine-transformed data for removal.

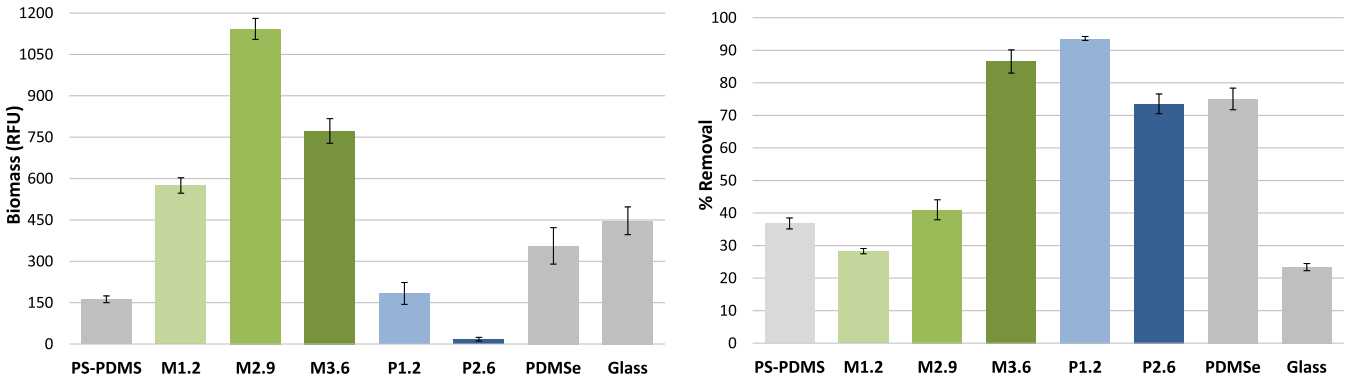

Figure 5. Density of attached *U. linza* spores after 45 min settlement on PS-PDMS morpholine amine coatings (left) and percent removal of 7-day-old sporelings due to a water jet impact pressure of 55 kPa (right). Each point is the mean from 90 counts on three replicate slides (settlement) reported as relative fluorescence units (RFUs) and the mean removal of biomass from six replicate slides measured using a fluorescence plate reader (removal). Bars show 95% confidence limits for settlement and standard error of the mean derived from arcsine-transformed data for removal.

against *N. incerta*, the morpholine coatings performed no better than the PS-PDMS control. Coatings P1.2 (226 cells/mm^2) and P2.6 (95 cells/mm^2) somewhat mitigated settlement compared to the control (292 cells/mm^2), with coating P2.6 reducing settlement by 67%. In removal assays (Figure 4), none of the coatings improved fouling release, with removal for all coatings below 25%. The only surface showing greater than 50% removal was the control glass slide, which indicates that the PS-PDMS-based surfaces were likely too hydrophobic for removal. With higher morpholine attachment, there was an increase in removal, from zero for coating M1.2 to 10% for coating M3.6 (Figure 4), but as seen in Figure S3, the number of cells retained on the surface after removal experiments were not statistically different (272 and 246 cells/mm^2, respectively).

Against *N. incerta*, modification with morpholine did not have any influence on antifouling or fouling-release properties. In settlement assays, morpholine coatings showed no improvement over the control, despite the fact that they all had lower contact angles. Previous studies have shown that *N. incerta* settlement and removal depend strongly on surface wettability, so it is interesting that, despite having similar contact angles, coatings P2.6 and M3.6 have such different success in preventing settlement. In removal experiments, none of the coatings showed improvement compared to the unfunctionalized PS-PDMS and PDMSe controls. In fact, the best performance was from the glass slide, a hydrophilic surface. Considering the general settlement and removal behavior of *N. incerta*, it is unsurprising that surfaces mostly composed of PDMS did not perform well. Likely, the loading of the hydrophilic group was too low to have a meaningful effect against diatoms.

U. linza is a common soft macrofouler found on ships' hulls and other submerged structures. Its settlement is governed by a motile zoospore, 4−8 μm in size, that actively chooses a settlement site based on cues such as wettability, topography, and surface charge.[74] Once a settlement site is chosen, the spore releases its adhesive and germinates into a nonmotile sporeling (young plant) that grows in length and is anchored to the surface by a rhizoid.[75,76] *U. linza* zoospores have previously demonstrated a tendency to favor settlement on hydrophobic rather than hydrophilic surfaces.[74] Interestingly, their primary adhesive has been shown to preferentially wet hydrophilic surfaces, ultimately leading to stronger adhesion.[77] In general, sporelings exhibit weaker adhesion to PDMS-based surfaces in fouling-release assays.[63,66] Zoospores of *U. linza* were exposed to surfaces for 45 min to evaluate the coatings' resistance to settlement. Functionalization with morpholine worsened the coatings' ability to resist settlement, with 4−7 times greater spore density compared to the unfunctionalized PS-PDMS control. Coating P1.2 showed similar performance to the unfunctionalized PS-PDMS control, while P2.6 was the only coating to perform better, reducing settlement almost 10 times in comparison to the control. After 7 days, biomass

https://doi.org/10.1021/acs.biomac.1c01474
Biomacromolecules XXXX, XXX, XXX−XXX

trends were the same as initial settlement (Figures 5 and S4), with the greatest density of sporelings observed on the three morpholine coatings and the lowest density on coating P2.6, which can be seen in Figure 6, by the dense lawn of sporelings on coatings M1.2, M2.9, and M3.6.

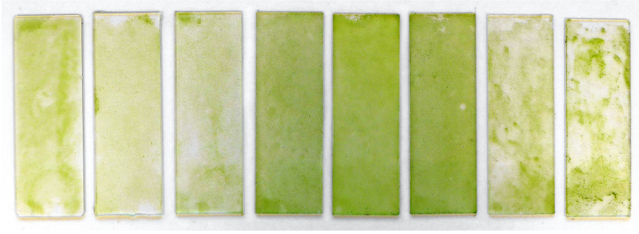

Figure 6. Typical growth of *U. linza* sporelings after 7 days on PS-PDMS morpholine amine coatings. From left: glass, PDMSe, PS-PDMS, M1.2, M2.9, M3.6, P1.2, and P2.6. All morpholine coatings show a dense lawn of sporelings, compared to the limited or patchy growth on PEG coatings and controls.

All loadings of morpholine amine had remarkably high settlement compared to the unfunctionalized PS-PDMS and PDMSe controls. The similar wettability of M3.6 and the PEG coatings indicates that there is a more complex interaction occurring that makes the morpholine surface more attractive to *U. linza* spores. One hypothesis for this behavior was the potential for protonation of the tertiary amine, which could generate a positive charge and act as a hydrogen bond donor. Charge is known to play a role in antifouling performance, with positively charged surfaces attracting the negatively charged *U. linza* spore.[26,78−80] This hypothesis was explored using a tertiary amide structure, and ultimately proved incorrect, as demonstrated in the subsequent coating set described in the following sections.

The greater biomass production (5754 RFU) on M3.6 than either PEG coatings (964 and 2277 RFU) was likely a result of the much higher spore settlement on the surface (see Figure S4). Despite this, performance in removal assays showed coating M3.6 to have fouling-release potential. After exposure to a 55 kPa water jet, coating M3.6 showed a 2-fold improvement in percent sporeling removal (86.8%) with respect to the unfunctionalized PS-PDMS control (36.8%) and showed performance similar in range to the two PEG coatings (93.6 and 73.6%). M1.2 and M2.9 performed similarly or worse compared to the control, indicating a loading threshold required to show effectiveness as a fouling-release material. M3.6 had similar fouling-release performance to the two PEG coatings, which aligns with its similar contact angle behavior, despite their lower wt % loading owing to the more compact structure of the morpholine. Overall, the M3.6 coating is not a suitable antifouling coating, as it cannot effectively prevent settlement on its surface. This coating type would be more appropriate as a strictly fouling-release surface in which hydrodynamic shear could be applied to induce the removal of fouling buildup.

Morpholine Amide Coating Set. *Material Synthesis and Coating Preparation.* To eliminate the ability to form a charge or act as a hydrogen bond donor, the morpholine amine group was modified to an N-substituted morpholine amide structure. In addition, two different lengths of PEG, a two-to-three unit PEG, to serve as 1:1 molar equiv to the small-molecule morpholine, and the previously used longer-chain seven-to-eight unit PEG, were included as controls. Modification of the PS-PDMS backbone was again done using a thiol−ene click reaction to pendant vinyl groups on the PDMS block. Thiol-bearing small molecules were synthesized for the two morpholine structures, as well as the two lengths of PEG. Functionalization efficiency with the amide (AMD) was considerably higher than that with the amine (AMN), with percent functionalization generally ranging from 80 to 100%. The resulting materials are detailed in Table 2, with their corresponding sample codes, this time corresponding to the weight percent of the hydrophilic group in the coating. Coatings were constructed as before on a base layer of SEBS using the same procedure as described above.[55,62]

Surface Characterization. Captive bubble contact angles were measured over a 7 day period to evaluate how backbone modification affected surface wettability (Figure 7). As before,

Table 2. Polymer Functionalization and Corresponding Sample Codes for PS-PDMS Morpholine Amide Coatings

code	side group	backbone structure	mol % vinyl[a]	mol % side group[a]	wt %[b]	coating wt %[c]
AMD-3.9	morpholine amide	diblock	3.24	2.59	4.3	3.9
		triblock	3.29	2.14	3.5	
AMD-7.4	morpholine amide	diblock	5.05	4.96	7.9	7.4
		triblock	5.05	4.40	7.0	
AMD-9.7	morpholine amide	diblock	6.65	6.08	9.9	9.7
		triblock	6.75	5.79	9.4	
AMN-4.5	morpholine amine	diblock	5.05	3.17	4.2	4.5
		triblock	5.05	3.55	4.7	
PEG150-3.2	PEG M_n = 150	diblock	3.24	1.65	2.8	3.2
		triblock	3.29	2.07	3.5	
PEG150-5.6	PEG M_n = 150	diblock	5.05	3.66	5.3	5.6
		triblock	5.05	3.67	5.9	
PEG150-8.3	PEG M_n = 150	diblock	6.65	5.39	8.9	8.3
		triblock	6.75	4.65	7.7	
PEG350-9.6	PEG M_n = 350	diblock	3.24	3.16	10.5	9.6
		triblock	3.29	2.63	8.7	

[a]Mole percent functionalized monomer units with respect to PDMS block calculated using ^{1}H NMR. [b]Weight percent functional group with respect to the total polymer molecular weight. [c]Coatings consist of 50/50 mixture diblock and triblock. Coating content calculated by averaging the diblock and triblock values.

https://doi.org/10.1021/acs.biomac.1c01474
Biomacromolecules XXXX, XXX, XXX−XXX

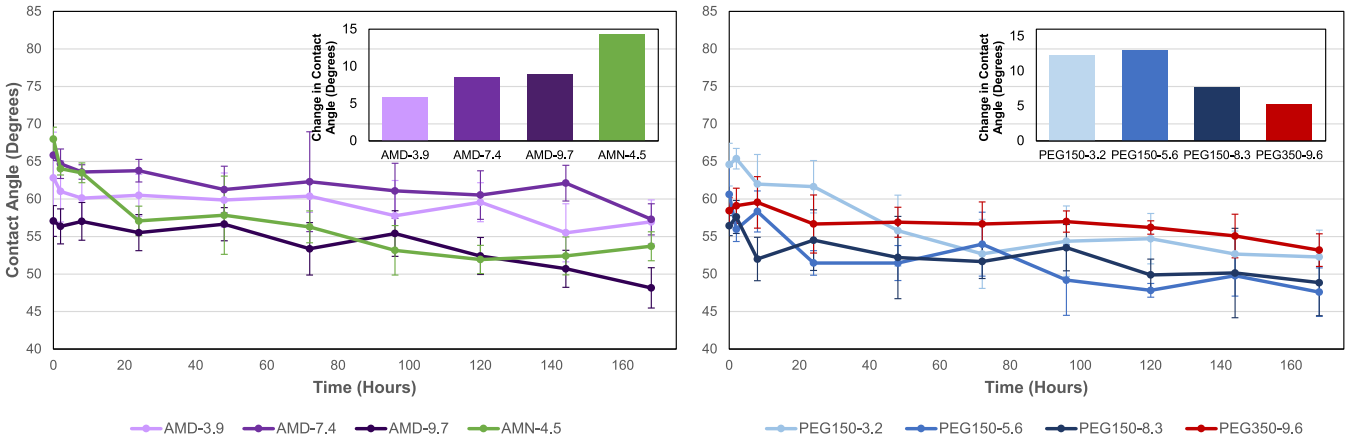

Figure 7. Captive bubble contact angles over a 7 day period for PS-PDMS morpholine amide (left) and PEG coatings (right). The inset indicates the total change in contact angle from the initial value for each coating. All coatings show a drop in contact angle, with AMN-4.5 and PEG150 coatings showing the most drastic changes. Error bars show standard deviation.

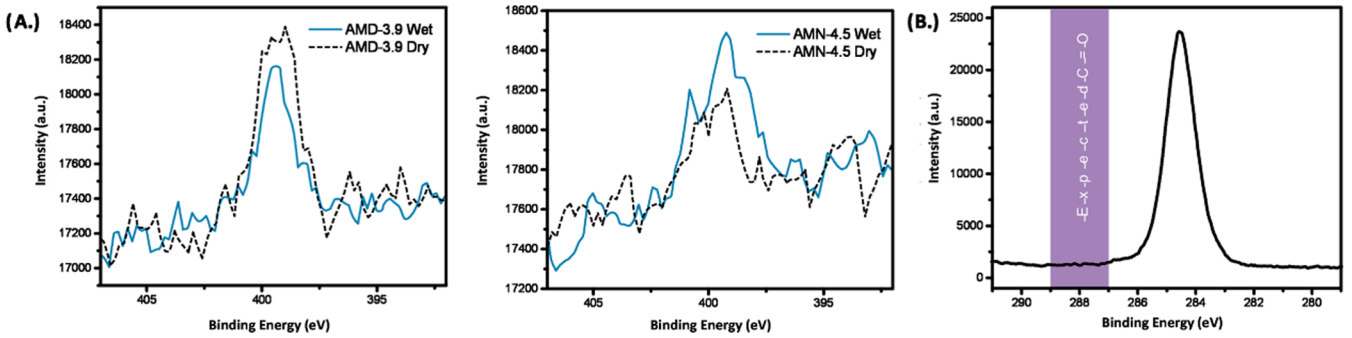

Figure 8. High-sensitivity XPS scans for N 1s in (A) AMD-3.9 (left) and AMN-4.5 (middle) coatings: measured in the dry state (dashed line) and after immersion in water for 72 h (solid line). While the AMD coatings all show a drop in nitrogen peak intensity with immersion in water, AMN-4.5 shows an increase, similar to that observed with the previous coating set. (B) High-resolution XPS C 1s spectrum of AMD-9.7 (right). High-resolution scans of AMD-9.7 show no indication of the C═O bond at the surface.

all of the modified coatings had lower contact angles than the unfunctionalized PS-PDMS (98°). Upon prolonged exposure to water, all of the AMD coatings underwent a drop in contact angle of less than 10°. Coating AMN-4.5, functionalized with the amine structure, showed the highest initial contact angle (68°) but underwent a greater change while in contact with water, with a drop of almost 15°, similar to the behavior of coating M3.6 in the previous set. This indicates that the amine structure is undergoing more change at the surface upon exposure to water than its amide counterpart, through either hydration or surface rearrangement.

The shorter-chain PEG materials also displayed drops in contact angle. Initial contact angles followed loading trends, with PEG150-3.2 having the highest (65°) and PEG150-8.3 having the lowest (56°). All short-chain PEG coatings showed a drop in contact angle, although this was more pronounced for PEG150-3.2 and PEG150-5.6 than for PEG150-8.3, 13° versus 8°, resulting in similar ultimate contact angles for PEG150-5.6 and PEG150-8.3. Interestingly, PEG350-9.6, using the longer PEG length, had a similar initial contact angle (58°) to the PEG150 coatings but showed little change over the sampling period, only dropping by about 5°, the smallest change of all of the coatings. This trend is especially interesting because the polymer has a considerably higher loading of hydrophilic material by weight percent than either PEG150-3.2 or PEG150-5.6, and the lowest change in contact angle would indicate that it is not adsorbing water or rearranging as readily as the other coatings.

The composition of the coatings, from XPS survey scans, is detailed in Table S4, including coating composition in both the as-deposited state and after immersion in water. The theoretical content of each coating differs significantly from the experimental values, which again is attributed to the surface dominance of the PDMS block burying much of the polystyrene block. When comparing the composition of surfaces in the as-deposited state versus those exposed to water, there is a consistent trend toward an increase in the carbon content at the surface and decreases in the oxygen and silicon contents, which is consistent with the surface composition shifting from mainly the PDMS backbone to more of the side groups presenting at the surface. The magnitude of the change is greater for the morpholine amide coatings, which is of note considering that the AMD coatings' contact angles did not change as much as the PEG150. This may indicate that while the surface of the morpholine coatings is rearranging, they are not hydrating as readily as the PEG coatings.

Survey XPS scans show no evidence of nitrogen at the surface of coatings, but high sensitivity nitrogen scans show the presence of nitrogen for the AMD coatings and AMN-4.5 (Figure 8). There is a greater nitrogen signal for the AMD coatings than for AMN-4.5, indicating that the morpholine amide is better at surface segregating than its amine

https://doi.org/10.1021/acs.biomac.1c01474
Biomacromolecules XXXX, XXX, XXX−XXX

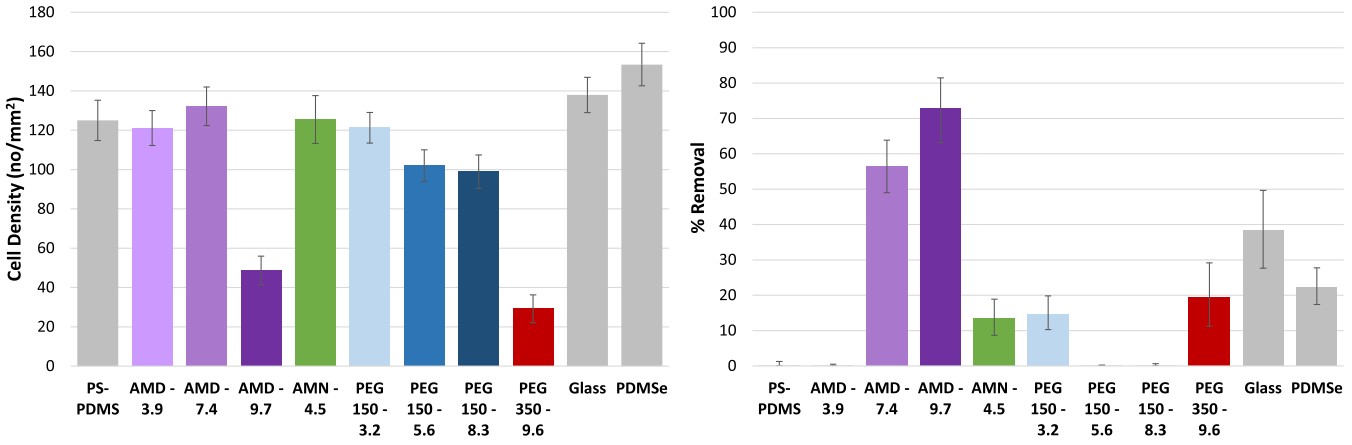

Figure 9. Density of attached *N. incerta* cells after 2 h (left) and percent removal due to a shear stress of 32 Pa (right) on amide coatings. Each point is the mean from 90 counts from three replicate slides for settlement. Bars show 95% confidence limits for settlement and 95% confidence limits derived from arcsine-transformed data for removal.

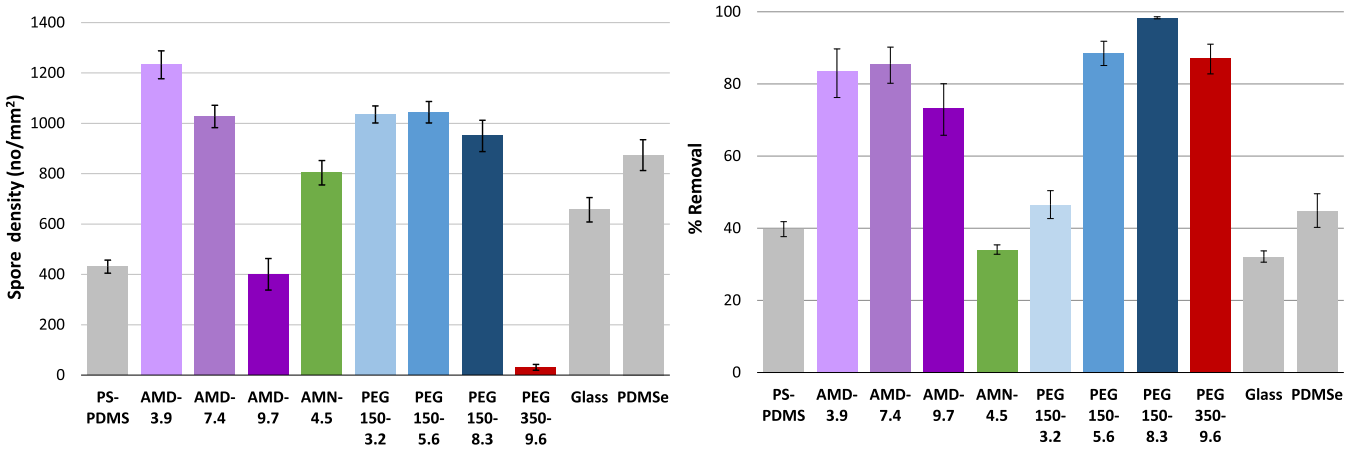

Figure 10. Densities of attached *U. linza* spores after 45 min settlement (left) and percent removal of 7-day-old sporelings due to an impact pressure of 42 Pa (left). Each point is the mean from 90 counts on three replicate slides for settlement and the percent removal of biomass from six replicate slides measured using a fluorescence plate reader for removal. Bars show 95% confidence limits for settlement and standard error of the mean derived from arcsine-transformed data for removal.

counterpart. This aligns with the contact angle data, in which AMD coatings all had lower initial contact angles than coating AMN-4.5. Comparing the magnitude of the nitrogen signals between the wet and dry, AMD coatings all show a decrease in signal after immersion in water, while AMN-4.5 shows an increase, the same as was observed in the previous coating set. No evidence of the amide carbonyl is visible in high-resolution C 1s scans, which would generally appear at a binding energy of 288 eV. The C−Si signal dominates again because the morpholine loading is quite low in comparison to the backbone, and the lower pass energy used for high-resolution scans limits the sensitivity.

The surface roughness of these coatings is detailed in Table S5. A higher-boiling-point cosolvent was chosen to minimize coating roughness compared to the previous coating set, resulting in greatly reduced roughness values, between 1.5 and 2 μm. Likewise, all coatings had maximum feature heights falling between 20 and 30 μm. Only coating AMD-9.7 had a roughness value below 1 μm and a maximum feature height of only about 17 μm. Coating morphologies were generally inconsistent between coatings, with no direct cause being evident, which can be seen in the surface morphology shown in the images in Figure S6. Spray coating conditions for all coatings were the same, and all materials showed similar solubility in the deposition solvent mixture, but coatings were deposited on different days and fluctuations in humidity and temperature could have played a role, which may explain the anomalous morphology. The differences in roughness and feature sizes may lead to differences in performance, particularly for the smoother AMD-9.7, as surface texture is known to affect the behavior of fouling organisms; however, its effect, if any, would be minimal at these length scales as recorded in the previous literature with similar coating systems.[81−87]

Fouling Assays. The antifouling and fouling-release character of coatings were again evaluated against the diatom *N. incerta* and the marine alga *U. linza*. Diatoms were settled on surfaces over a 2 h period. As seen in Figures 9 and S7, the performances of AMD-3.9 and AMD-7.4 were the same as that of the unfunctionalized control (125 cells/mm^2), while AMD-9.7 showed a more than 60% reduction in settlement (49 cells/mm^2). AMN-4.5 also performed the same as the control, showing no benefit in preventing settlement but not promoting it. The PEG coatings also showed a dependence on the loading, but the effect was not as pronounced. Coating PEG150-3.2 performed no better than the control, while

https://doi.org/10.1021/acs.biomac.1c01474
Biomacromolecules XXXX, XXX, XXX−XXX

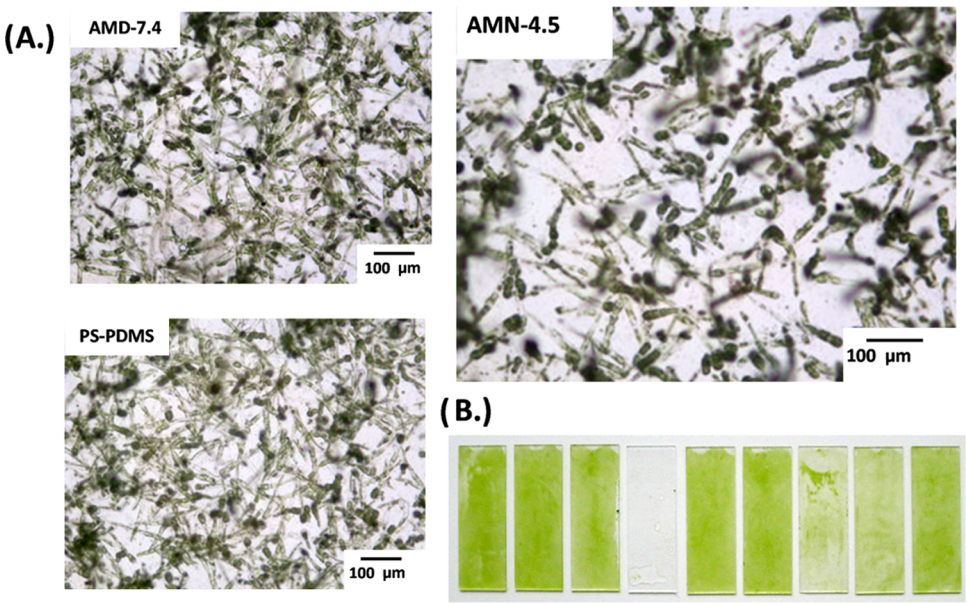

Figure 11. Typical *U. linza* sporeling growth on coatings. (A) AMN-4.5, AMD-7.4, and unfunctionalized PS-PDMS showing normal germination and proliferation with no indications of sporeling death or pseudo-settlement as would be expected for an algicidal surface. (B) Image showing *U. linza* sporeling growth on full coating substrates. From left: PEG150-3.2, PEG150-5.6, PEG150-8.3, PEG350-9.6, AMD-3.9, AMD-7.4, AMD-9.7, PS-PDMS, and AMN-4.5.

coatings PEG150-5.6 and PEG150-8.3 showed a 20% reduction in settlement. In contrast, coating PEG350-9.6 showed the best performance overall (29 cells/mm^2), reducing settlement by over 75%. This performance was quite like coating AMD-9.7, which had a similar weight fraction loading of the hydrophilic group.

Out of all of the coatings tested, the highest removal of *N. incerta* cells was from coatings AMD-7.4 and AMD-9.7, which had 56% and 73% removal, respectively, higher than all other coatings and control slides. Coating AMN-4.5 had limited removal (13%), similar to coatings PEG150-3.2 (15%) and PEG350-9.6 (19%), which were less than the removal from the glass reference slide. Meanwhile, the control and coatings AMD-3.9, PEG150-5.6, and PEG150-8.3 retained all settled diatoms, with no organisms removed from their surfaces. While the percent removal from PEG350-9.6 was the same as from coatings AMN-4.5 and PEG150-3.2, it had considerably less diatoms retained on it after the removal experiments, indicating its superior performance as an antifouling material. In fact, while it had almost 3 times lower percent removal than coating AMD-7.4, it ultimately had 50% less retained diatoms on the surface. Considering nearly comparable settlement and a 3-fold higher removal, the AMD-9.7 clearly outshines even the best PEG (PEG-9.6) coating in the overall foulant resistance.

The *U. linza* assays also show promising results but with distinct differences in performance compared to *N. incerta*. As seen in Figures 10 and S8, coating AMD-9.7 (400 spores/mm^2) showed settlement equivalent to that of the control (431 spores/mm^2). The only coating that performed better was PEG350-9.6 (31 spores/mm^2), which showed over 10 times improvement in resistance to settlement. Coating AMD-3.9 had three times greater settlement (1232 spores/mm^2) than the control, while AMD-7.4 and AMN-4.5 were approximately double that of the control. The PEG coatings showed somewhat surprising results. For PEG150 coatings, PEG loading had no influence on settlement, with all three coatings having settlement in the range of 1000 spores/mm^2. Previously, this system using a seven-to-eight unit PEG has shown improved resistance to *U. linza* spore settlement, as demonstrated by coating PEG350-9.6, but the use of the shorter PEG resulted in increased settlement compared to the unfunctionalized backbone.

In general, *U. linza* growth after a 7 day period resembled the trends seen in initial settlement, with PEG350-9.6 maintaining the greatest resistance to growth, AMD-9.7 performing equivalently to the control, and all other coatings having greater spore densities. While it was hypothesized that the amine's ability to protonate and form a positive charge could give the surface algicidal properties, as was shown with poly(2-(dimethylamino)ethyl methacrylate) (PDMAEMA) polymer brushes,[26] there was no evidence of this on coating AMN-4.5. Images in Figure 11 demonstrate normal growth, like the growth observed on coating AMD-7.4 and unfunctionalized PS-PDMS, and no evidence of pseudo-settlement or spore death, indicating that the amine surface has no noticeable algicidal properties.

In removal assays utilizing a 42 Pa shear stress, the performance of all of the morpholine amide coatings was similar, with 70−85% removal and comparable to the PEG coatings. The PS-PDMS control only had 40% removal, and therefore, the incorporation of the morpholine amide essentially doubled removal. Coating AMN-4.5, in contrast, showed slightly worse performance than the control, with only 34% removal. For PEG-containing coatings, increased removal correlated with greater loading. Coating PEG150-3.2 was only slightly better than the control, but both PEG150-5.6 and PEG150-8.3 had over 90% removal of sporelings. PEG350-9.6 also showed high sporeling removal (87%).

Overall, in settlement assays, performance strongly depended on the loading of the morpholine amide for both *N. incerta* and *U. linza*. AMD-9.7 showed improved resistance to *N. incerta* settlement compared to the control. Its performance was equivalent to the control against *U. linza*, while lower

https://doi.org/10.1021/acs.biomac.1c01474
Biomacromolecules XXXX, XXX, XXX−XXX

loadings of morpholine promoted spore settlement. It is important to recall that while AMD-9.7 had a contact angle value of ∼10° lower than the other two AMD coatings, it displayed similar wettability behavior to the PEG150 coatings. However, the antifouling and fouling-release performances of AMD-9.7, against both *N. incerta* and *U. linza,* were markedly better than that of the PEG150, indicating that it was not strictly wettability controlling performance. XPS data showed differences in surface composition; so, although the wettability behaviors are similar, there is likely more hydrophilic groups at the surface in coating AMD-9.7. It also had a lower roughness than all other coatings, and *U. linza* is known to settle preferentially on rougher surfaces;[75] however, the effect of roughness would be minimal at these reported values according to the previous literature.[85−87] For both species, the trend toward better resistance to settlement with higher functionalization indicates that increasing the loading of morpholine amide would likely lead to further improvement in performance as an antifouling material.

Comparison of the amide with the amine form of the morpholine showed little difference in terms of initial attachment for *N. incerta* and slightly improved performance at similar loading percentages for *U. linza*, although this performance was still worse than the control. This increased settlement on the amide is contrary to what was expected, based on the hypothesis that the higher settlement of *U. linza* spores was a result of protonation of the tertiary amine, indicating that the increase in *U. linza* settlement had other causes. The captive bubble contact angles varied little between the coatings, and therefore, the effects of surface energy were not responsible for the majority of the differences in initial algal attachment.

In removal experiments, the morpholine amide improved performance against both species. For *N. incerta*, this improvement depended on loading. AMD-7.4 and AMD-9.7 showed the highest removal, markedly better than all of the PEG coatings. The adhesion strength of *N. incerta* diatoms is known to be strongly influenced by the surface hydrophilicity, with strong adhesion to hydrophobic surfaces like silicone elastomers.[73] It is unsurprising that the morpholine amide coating improved removal considerably compared to the unfunctionalized PS-PDMS control, but unexpected that AMD-7.4 performed significantly better than AMD-3.9, considering the similarity in their wettability. Additionally, it performed significantly better than the PEG coatings, despite exhibiting higher contact angles. Likely, there may be a structural characteristic of the morpholine amide that creates a surface where the diatoms cannot form a strong adhesive bond. Recent studies of zwitterionic polymer coatings with a variety of quaternary amine cations also noted the superior resistance to diatom attachment in coatings containing the morpholinium cation.[88] Against *U. linza*, loading did not play a role in the fouling release of AMD coatings, while there was a dependence on loading for the PEG150 coatings. At the lowest loading, the morpholine was much more effective at improving fouling release than the PEG150 counterpart. Considering the higher contact angles of the morpholine amide coating, this may again point to a unique attribute of the morpholine amide structure for use in marine fouling-release coatings.

It was hypothesized that the morpholine amine structure could be promoting settlement based on its ability to protonate. The reality is likely more complex. While the amine form did still have a higher settlement of spores than the control, all surfaces except for AMD-9.7 and PEG350-9.6 also promoted settlement, which indicates that charge was not the most likely factor influencing this settlement behavior. Additionally, spore growth was normal on coating AMN-4.5, precluding the notion that the amine surfaces possess algicidal properties. In fact, the amide, which cannot protonate, was superior to the amine as a fouling-release material, with at least double the density of organisms remaining on the amine coating compared to the equivalently loaded amide coating in both removal experiments. From the XPS, though, the population of morpholine at the surface is still quite low. Inducement of algicidal properties of this surface might be achieved with greater loading of morpholine.

Although similar in structure to the morpholine amine, the morpholine amide shows more potential as a fouling-release material. Uniquely, the morpholine amide improved performance against both species of foulers tested here, indicating that it may offer more utility as a hydrophilic component for building a broad-spectrum fouling-release coating than either morpholine amine or PEG. As an antifouling material, its influence is more modest. Against *N. incerta* only, the highest loading of morpholine amide was able to prevent settlement compared to that of the control, while against *U. linza*, AMD-9.7 performed equivalently to the control. Based on the fouling-release performance demonstrated in this study, morpholine amide is a promising material, but further study of its antifouling characteristics, particularly at higher loadings, is required for better understanding of its contributions to antifouling performance.

While the goal of this study was to investigate the performance of the morpholine amide, an interesting result emerged related to the length of PEG. Against *N. incerta*, coating PEG350-9.6 resisted settlement to a greater extent than any of coatings tested, while coating PEG150-8.3, which had a similar weight percent loading of PEG, but a shorter length, performed only marginally better than the control. And against *U. linza*, PEG150 coatings all promoted settlement compared to the control, while PEG350-9.6 had more than 30 times lower settlement. The previous coating sets, P2.6 and P1.2 (which would approximate PEG350-8.7 and PEG350-3.9, respectively), did not promote settlement and performed better or equivalently to the control; so, the slight discrepancy in loading does not account for the differences in behavior. This is especially interesting considering PEG350-9.6 had the highest ultimate contact angle of all of the PEG coatings, which would indicate that it was the least hydrophilic. All coatings had similar surface roughnesses and feature sizes, indicating that the morphology was not the contributing factor either. Molecular composition also showed little difference, with PEG350-9.6 having a composition falling somewhere between that of PEG150-5.6 and PEG150-8.3. The only real difference was the length of the PEG chains. Combined with the higher contact angle of coating PEG350-9.6 and the promotion of settlement on the morpholine surfaces, this result may point to the importance of the side group length.

In the study of protein-resistant surfaces, PEG is thought to function in two ways: formation of a water layer and steric repulsion due to chain flexibility.[11] Formation of a hydration layer occurs because of PEG's ability to strongly hydrogen-bond with water, creating a physical barrier to the adsorption of proteins, while steric repulsion is thought to prevent protein adsorption because of the compression and conformational entropy loss that would occur upon adsorption.[89] Both long-

https://doi.org/10.1021/acs.biomac.1c01474
Biomacromolecules XXXX, XXX, XXX−XXX

and short-chain PEGs are capable of forming hydrogen bonds and a subsequent water layer, but longer-chain PEGs are thought to also work because of steric repulsion of proteins.[90] The lower contact angles of the PEG150 coatings indicate that water adsorption was occurring. So, the settlement results suggest that the formation of a water barrier was not the controlling factor in the performance of these coatings. This result may point to a greater influence by the steric repulsion model for PEG in the prevention of marine foulant settlement, which makes sense given the performance of most morpholine coatings was in general more similar to that of the PEG150 coatings. Because of the complexity of this system, from the use of a block copolymer to PEG being tethered to the PDMS block in low loading percentages, it is difficult to quantify the contribution from this steric factor. Ultimately, further investigation of the surface hydration and a more targeted study on the effects of PEG length and loading in the PS-PDMS system should be undertaken to help elucidate these differences in behavior, as it will be important for developing effective antifouling and fouling-release surfaces in the future.

CONCLUSIONS

In this study, two structural analogues of the small-molecule morpholine were incorporated into an antifouling and fouling-release PS-PDMS block copolymer system, and its coatings were evaluated for performance against two soft fouling species. Two sets of coatings were investigated, the first focusing on the N-substituted amine form of morpholine and the second looking at the N-substituted amide. The morpholine amine indicated promising behavior as a fouling-release material against *U. linza* but promoted settlement of its spores, and against *N. incerta*, modification with the morpholine amine had no effect on settlement or adhesion.

The morpholine amide demonstrates improved fouling release against both organisms at comparable loading and good antifouling performance against *N. incerta* at the highest loading. Overall, the morpholine amide at higher loading, with significantly lower final cell/spore densities, markedly improves fouling resistance against both organisms. This is notable, as *U. linza* and *N. incerta* usually have opposite adhesion characteristics, and coatings with effectiveness against both are unusual. Although the morpholine does add hydrophilicity to the surface, considerably lowering the contact angle, that does not solely explain the performance improvement and particularly against *N. incerta*, there may be some inherent characteristic that limits diatom adhesion. Interestingly, the poor antifouling behavior against *U. linza* did not result from the tertiary amine structure as lower loadings of the morpholine amide also increased the settlement of *U. linza* spores on surfaces compared to that of the control. Additionally, there was an interesting trend in the behavior of organisms on the PEG coatings. The longer length performed considerably better than its shorter counterpart, even when loaded at a similar weight percent, pointing to the importance of the steric factor in addition to wettability. Importantly, at higher loading percentages, the much smaller and less hydrophilic morpholine amide coatings outperformed even the longest PEG coatings against *N. incerta*. This suggests that in addition to steric and wettability factors, other factors unique to the chemical structure of the morpholine amide are influencing fouling inhibition. Future studies to examine surface characteristics, such as the formation of a hydration layer and water structuring of both the amide and the different PEG lengths, may elucidate the exact structural origin of this behavior.

Ultimately, the N-substituted morpholine amide is a more promising addition for PDMS-based fouling-release coatings than the amine, and its efficacy against both *U. linza* and *N. incerta* offers a unique advantage compared to PEG. Importantly, the morpholine amide group is also much smaller than its counterpart PEG, allowing for the incorporation into more elegant and compact systems such as peptoids and artificial polypeptides. Additional study of the antifouling performance for the morpholine amide structure is required to better assess its capabilities to prevent surface settlement, but the demonstrated fouling-release efficacy against both species of foulers warrants its further exploration as a compact alternative to PEG.

ASSOCIATED CONTENT

Supporting Information

The Supporting Information is available free of charge at https://pubs.acs.org/doi/10.1021/acs.biomac.1c01474.

Details of surface characterization methods; GPC and ^{1}H NMR characterization data for block copolymer and its derivatives; roughness ratios calculated from profilometry; complete XPS surface compositions; and additional fouling assay data (PDF)

AUTHOR INFORMATION

Corresponding Author

Christopher K. Ober − *Department of Materials Science and Engineering, Cornell University, Ithaca, New York 14853, United States;* orcid.org/0000-0002-3805-3314; Email: cko3@cornell.edu

Authors

Amanda K. Leonardi − *Department of Chemistry and Chemical Biology, Cornell University, Ithaca, New York 14853, United States*

Riddhiman Medhi − *Department of Materials Science and Engineering, Cornell University, Ithaca, New York 14853, United States;* orcid.org/0000-0002-2368-2468

Aria Zhang − *Department of Materials Science and Engineering, Cornell University, Ithaca, New York 14853, United States*

Nilay Düzen − *Department of Materials Science and Engineering, Cornell University, Ithaca, New York 14853, United States*

John A. Finlay − *School of Natural and Environmental Sciences, Newcastle University, Newcastle upon Tyne NE1 7RU, U.K.*

Jessica L. Clarke − *School of Natural and Environmental Sciences, Newcastle University, Newcastle upon Tyne NE1 7RU, U.K.*

Anthony S. Clare − *School of Natural and Environmental Sciences, Newcastle University, Newcastle upon Tyne NE1 7RU, U.K.*

Complete contact information is available at: https://pubs.acs.org/10.1021/acs.biomac.1c01474

Author Contributions

The manuscript was written through contributions of all authors. All authors have given approval to the final version of the manuscript.

https://doi.org/10.1021/acs.biomac.1c01474
Biomacromolecules XXXX, XXX, XXX−XXX

Notes

The authors declare no competing financial interest.

■ ACKNOWLEDGMENTS

This research was primarily supported by the Office of Naval Research awards N000141612960 and N000141612988. This work made use of the Cornell Center for Materials Research Shared Facilities, which were supported through the NSF MRSEC program (DMR-1719875). This work made use of the Cornell University NMR Facility, which was supported, in part, by the NSF through MRI award CHE-1531632. The authors would also like to thank Prof. Rachel Segalman and her students (UCSB) for their fruitful discussions related to this work.

■ REFERENCES

(1) Schultz, M. P. Effects of Coating Roughness and Biofouling on Ship Resistance and Powering. *Biofouling* **2007**, *23*, 331−341.
(2) Schultz, M. P.; Bendick, J. A.; Holm, E. R.; Hertel, W. M. Economic Impact of Biofouling on a Naval Surface Ship. *Biofouling* **2011**, *27*, 87−98.
(3) Donnelly, B.; Bedwell, I.; Dimas, J.; Scardino, A.; Tang, Y.; Sammut, K. Effects of Various Antifouling Coatings and Fouling on Marine Sonar Performance. *Polymers* **2019**, *11*, No. 663.
(4) Woods Hole Oceanographic Institute (WHOI). The History of the Prevention of Fouling. *Marine Fouling and Its Prevention*; George Banta Publishing Co.: Menasha, Wisconsin, 1952; pp 211−222.
(5) Readman, J. W. Development, Occurrence and Regulation of Antifouling Paint Biocides: Historical Review and Future Trends. *Handbook of Environmental Chemistry*; Springer-Verlag: Berlin, 2006; Vol. *5*, pp 1−15.
(6) Champ, M. A. Economic and Environmental Impacts on Ports and Harbors from the Convention to Ban Harmful Marine Anti-Fouling Systems. *Mar. Pollut. Bull.* **2003**, *46*, 935−940.
(7) Matthiessen, P.; Reed, J.; Johnsonà, M. Sources and Potential Effects of Copper and Zinc Concentrations in the Estuarine Waters of Essex and Suffolk, United Kingdom. *Mar. Pollut. Bull.* **1999**, *38*, 908−920.
(8) Ytreberg, E.; Karlsson, J.; Eklund, B. Comparison of Toxicity and Release Rates of Cu and Zn from Anti-Fouling Paints Leached in Natural and Artificial Brackish Seawater. *Sci. Total Environ.* **2010**, *408*, 2459−2466.
(9) Thomas, K. The Environmental Fate and Behaviour of Antifouling Paint Booster Biocides: A Review. *Biofouling* **2001**, *17*, 73−86.
(10) Oliveira, I. B.; Groh, K. J.; Schönenberger, R.; Barroso, C.; Thomas, K. V.; Suter, M. J. F. Toxicity of Emerging Antifouling Biocides to Non-Target Freshwater Organisms from Three Trophic Levels. *Aquat. Toxicol.* **2017**, *191*, 164−174.
(11) Chen, S.; Li, L.; Zhao, C.; Zheng, J. Surface Hydration: Principles and Applications toward Low-Fouling/Nonfouling Biomaterials. *Polymer* **2010**, *51*, 5283−5293.
(12) Krishnan, S.; Weinman, C. J.; Ober, C. K. Advances in Polymers for Anti-Biofouling Surfaces. *J. Mater. Chem.* **2008**, *18*, 3405−3413.
(13) Kuliasha, C. A.; Finlay, J. A.; Franco, S. C.; Clare, A. S.; Stafslien, S. J.; Brennan, A. B. Marine Anti-Biofouling Efficacy of Amphiphilic Poly(Coacrylate) Grafted PDMSe: Effect of Graft Molecular Weight. *Biofouling* **2017**, *33*, 252−267.
(14) Zhang, Y.; Hu, H.; Pei, X.; Liu, Y.; Ye, Q.; Zhou, F. Polymer Brushes on Structural Surfaces: A Novel Synergistic Strategy for Perfectly Resisting Algae Settlement. *Biomater. Sci.* **2017**, *5*, 2493−2500.
(15) Martinelli, E.; Gunes, D.; Wenning, B. M.; Ober, C. K.; Finlay, J. A.; Callow, M. E.; Callow, J. A.; Di Fino, A.; Clare, A. S.; Galli, G. Effects of Surface-Active Block Copolymers with Oxyethylene and Fluoroalkyl Side Chains on the Antifouling Performance of Silicone-Based Films. *Biofouling* **2016**, *32*, 81−93.
(16) Wenning, B. M.; Martinelli, E.; Mieszkin, S.; Finlay, J. A.; Fischer, D.; Callow, J. A.; Callow, M. E.; Leonardi, A. K.; Ober, C. K.; Galli, G. Model Amphiphilic Block Copolymers with Tailored Molecular Weight and Composition in PDMS-Based Films to Limit Soft Biofouling. *ACS Appl. Mater. Interfaces* **2017**, *9*, 16505−16516.
(17) Hawkins, M. L.; Faÿ, F.; Réhel, K.; Linossier, I.; Grunlan, M. A. Bacteria and Diatom Resistance of Silicones Modified with PEO-Silane Amphiphiles. *Biofouling* **2014**, *30*, 247−258.
(18) Faÿ, F.; Hawkins, M. L.; Rehel, K.; Linossier, I.; Grunlan, M. A. Non-Toxic, Antifouling Silicones with Variable PEO − Silane Amphiphile Content. *Green Mater.* **2016**, *4*, 53−62.
(19) Webster, D. C.; Bodkhe, R. B. Functionalized Silicones with Polyalkylene Oxide Side Chains. WO2013/052181 A2, 2013.
(20) Galhenage, T. P.; Webster, D. C.; Moreira, A. M. S.; Burgett, R. J.; Stafslien, S. J.; Vanderwal, L.; Finlay, J. A.; Franco, S. C.; Clare, A. S. Poly(Ethylene) Glycol-Modified, Amphiphilic, Siloxane−Polyurethane Coatings and Their Performance as Fouling-Release Surfaces. *J. Coat. Technol. Res.* **2017**, *14*, 307−322.
(21) Hoang Thi, T. T.; Pilkington, E. H.; Nguyen, D. H.; Lee, J. S.; Park, K. D.; Truong, N. P. The Importance of Poly(Ethylene Glycol) Alternatives for Overcoming PEG Immunogenicity in Drug Delivery and Bioconjugation. *Polymers* **2020**, *12*, No. 298.
(22) Qi, Y.; Chilkoti, A. Protein-Polymer Conjugation-Moving beyond PEGylation. *Curr. Opin. Chem. Biol.* **2015**, *28*, 181−193.
(23) Camós Noguer, A.; Olsen, S. M.; Hvilsted, S.; Kiil, S. Long-Term Stability of PEG-Based Antifouling Surfaces in Seawater. *J. Coat. Technol. Res.* **2016**, *13*, 567−575.
(24) Ulbricht, J.; Jordan, R.; Luxenhofer, R. On the Biodegradability of Polyethylene Glycol, Polypeptoids and Poly(2-Oxazoline)s. *Biomaterials* **2014**, *35*, 4848−4861.
(25) Yandi, W.; Mieszkin, S.; di Fino, A.; Martin-Tanchereau, P.; Callow, M. E.; Callow, J. A.; Tyson, L.; Clare, A. S.; Ederth, T. Charged Hydrophilic Polymer Brushes and Their Relevance for Understanding Marine Biofouling. *Biofouling* **2016**, *32*, 609−625.
(26) Yandi, W.; Mieszkin, S.; Callow, M. E.; Callow, J. A.; Finlay, J. A.; Liedberg, B.; Ederth, T. Antialgal Activity of Poly(2-(Dimethylamino)Ethyl Methacrylate) (PDMAEMA) Brushes against the Marine Alga *Ulva*. *Biofouling* **2017**, *33*, 169−183.
(27) Higaki, Y.; Nishida, J.; Takenaka, A.; Yoshimatsu, R.; Kobayashi, M.; Takahara, A. Versatile Inhibition of Marine Organism Settlement by Zwitterionic Polymer Brushes. *Polym. J.* **2015**, *47*, 811−818.
(28) Bauer, S.; Arpa-Sancet, M. P.; Finlay, J. A.; Callow, M. E.; Callow, J. A.; Rosenhahn, A. Adhesion of Marine Fouling Organisms on Hydrophilic and Amphiphilic Polysaccharides. *Langmuir* **2013**, *29*, 4039−4047.
(29) Bodkhe, R. B.; Stafslien, S. J.; Cilz, N.; Daniels, J.; Thompson, S. E. M.; Callow, M. E.; Callow, J. A.; Webster, D. C. Polyurethanes with Amphiphilic Surfaces Made Using Telechelic Functional PDMS Having Orthogonal Acid Functional Groups. *Prog. Org. Coat.* **2012**, *75*, 38−48.
(30) Quintana, R.; Gosa, M.; Jańczewski, D.; Kutnyanszky, E.; Vancso, G. J. Enhanced Stability of Low Fouling Zwitterionic Polymer Brushes in Seawater with Diblock Architecture. *Langmuir* **2013**, *29*, 10859−10867.
(31) Xu, G.; Liu, P.; Pranantyo, D.; Xu, L.; Neoh, K. G.; Kang, E. T. Antifouling and Antimicrobial Coatings from Zwitterionic and Cationic Binary Polymer Brushes Assembled via "Click" Reactions. *Ind. Eng. Chem. Res.* **2017**, *56*, 14479−14488.
(32) Ventura, C.; Guerin, A. J.; El-Zubir, O.; Ruiz-Sanchez, A. J.; Dixon, L. I.; Reynolds, K. J.; Dale, M. L.; Ferguson, J.; Houlton, A.; Horrocks, B. R.; Clare, A. S.; Fulton, D. A. Marine Antifouling Performance of Polymer Coatings Incorporating Zwitterions. *Biofouling* **2017**, *33*, 892−903.
(33) Bauer, S.; Finlay, J. A.; Thomé, I.; Nolte, K.; Franco, S. C.; Ralston, E.; Swain, G. E.; Clare, A. S.; Rosenhahn, A. Attachment of

https://doi.org/10.1021/acs.biomac.1c01474
Biomacromolecules XXXX, XXX, XXX−XXX

Algal Cells to Zwitterionic Self-Assembled Monolayers Comprised of Different Anionic Compounds. *Langmuir* **2016**, *32*, 5663−5671.
(34) Wang, H.; Zhang, C.; Wang, J.; Feng, X.; He, C. Dual-Mode Antifouling Ability of Thiol-Ene Amphiphilic Conetworks: Minimally Adhesive Coatings via the Surface Zwitterionization. *ACS Sustainable Chem. Eng.* **2016**, *4*, 3803−3811.
(35) Xie, Q.; Xie, Q.; Pan, J.; Ma, C.; Zhang, G. Biodegradable Polymer with Hydrolysis-Induced Zwitterions for Antibiofouling. *ACS Appl. Mater. Interfaces* **2018**, *10*, 11213−11220.
(36) Kourounakis, A. P.; Xanthopoulos, D.; Tzara, A. Morpholine as a Privileged Structure: A Review on the Medicinal Chemistry and Pharmacological Activity of Morpholine Containing Bioactive Molecules. *Med. Res. Rev.* **2020**, *40*, 709−752.
(37) Kumari, A.; Singh, R. K. Morpholine as Ubiquitous Pharmacophore in Medicinal Chemistry: Deep Insight into the Structure-Activity Relationship (SAR). *Bioorg. Chem.* **2020**, *96*, No. 103578.
(38) Tzara, A.; Xanthopoulos, D.; Kourounakis, A. P. Morpholine As a Scaffold in Medicinal Chemistry: An Update on Synthetic Strategies. *ChemMedChem* **2020**, *15*, 392−403.
(39) Rupak, K.; Vulichi, S. R.; Suman, K. Emphasizing Morpholine and Its Derivatives (Maid): Typical Candidate of Pharmaceutical Importance. *Int. J. Chem. Sci.* **2016**, *14*, 1777−1788.
(40) Saini, B.; Vaghani, D.; Khuntia, S.; Sinha, M. K.; Patel, A.; Pindoria, R. A Novel Stimuli-Responsive and Fouling Resistant PVDF Ultrafiltration Membrane Prepared by Using Amphiphilic Copolymer of Poly(Vinylidene Fluoride) and Poly(2-N-Morpholino)Ethyl Methacrylate. *J. Membr. Sci.* **2020**, *603*, No. 118047.
(41) Demirci, S.; Kinali-Demirci, S.; Jiang, S. A Switchable Polymer Brush System for Antifouling and Controlled Detection. *Chem. Commun.* **2017**, *53*, 3713−3716.
(42) Takahashi, H.; Nakayama, M.; Itoga, K.; Yamato, M.; Okano, T. Micropatterned Thermoresponsive Polymer Brush Surfaces for Fabricating Cell Sheets with Well-Controlled Orientational Structures. *Biomacromolecules* **2011**, *12*, 1414−1418.
(43) Duque-Sanchez, L.; Brack, N.; Postma, A.; Meagher, L.; Pigram, P. J. Engineering the Biointerface of Electrospun 3D Scaffolds with Functionalized Polymer Brushes for Enhanced Cell Binding. *Biomacromolecules* **2019**, *20*, 813−825.
(44) Duque-Sánchez, L.; Brack, N.; Postma, A.; Pigram, P. J.; Meagher, L. Optimisation of Grafting of Low Fouling Polymers from Three-Dimensional Scaffolds via Surface-Initiated Cu(0) Mediated Polymerisation. *J. Mater. Chem. B* **2018**, *6*, 5896−5909.
(45) Liu, J.; Shen, X.; Zhao, Y.; Chen, L. Acryloylmorpholine-Grafted PVDF Membrane with Improved Protein Fouling Resistance. *Ind. Eng. Chem. Res.* **2013**, *52*, 18392−18400.
(46) Xu, R.; Feng, Q.; He, Y.; Yan, F.; Chen, L.; Zhao, Y. Dual Functionalized Poly(Vinylidene Fluoride) Membrane with Acryloylmorpholine and Argatroban to Improve Antifouling and Hemocompatibility. *J. Biomed. Mater. Res., Part A* **2017**, *105*, 178−188.
(47) Shen, X.; Liu, J.; Feng, X.; Zhao, Y.; Chen, L. Preliminary Investigation on Hemocompatibility of Poly(Vinylidene Fluoride) Membrane Grafted with Acryloylmorpholine via ATRP. *J. Biomed. Mater. Res., Part A* **2015**, *103*, 683−692.
(48) He, Y.; Xu, L.; Feng, X.; Zhao, Y.; Chen, L. Dopamine-Induced Nonionic Polymer Coatings for Significantly Enhancing Separation and Antifouling Properties of Polymer Membranes: Codeposition versus Sequential Deposition. *J. Membr. Sci.* **2017**, *539*, 421−431.
(49) Callow, M. E.; Callow, J. A.; Pickett-Heaps, J. D.; Wetherbee, R. Primary Adhesion of *Enteromorpha* (Chlorophyta, Ulvales) Propagules: Quantitative Settlement Studies and Video Microscopy. *J. Phycol.* **1997**, *33*, 938−947.
(50) Starr, R.; Zeikus, J. UTEX − the culture collection of algae at the University of Texas at Austin. *J. Phycol.* **1993**, *29*, 1−106.
(51) Schultz, M. P.; Finlay, J. A.; Callow, M. E.; Callow, J. A. A Turbulent Channel Flow Apparatus for the Determination of the Adhesion Strength of Microfouling Organisms. *Biofouling* **2000**, *15*, 243−251.
(52) Finlay, J. A.; Callow, M. E.; Schultz, M. P.; Swain, G. W.; Callow, J. A. Adhesion Strength of Settled Spores of the Green Alga Enteromorpha. *Biofouling* **2002**, *18*, 251−256.
(53) Calabrese, D. R.; Wenning, B.; Finlay, J. A.; Callow, M. E.; Callow, J. A.; Fischer, D.; Ober, C. K. Amphiphilic Oligopeptides Grafted to PDMS-Based Diblock Copolymers for Use in Antifouling and Fouling Release Coatings. *Polym. Adv. Technol.* **2015**, *26*, 829−836.
(54) Wenning, B. M. Synthesis and Study of Functionalized Poly(Dimethyl Siloxane) Block Copolymers: Control of Surface Properties and Use in Antibiofouling Coatings. Cornell University, 2016.
(55) Weinman, C. J.; Finlay, J. A.; Park, D.; Paik, M. Y.; Krishnan, S.; Sundaram, H. S.; Dimitriou, M.; Sohn, K. E.; Callow, M. E.; Callow, J. A.; Handlin, D. L.; Willis, C. L.; Kramer, E. J.; Ober, C. K. ABC Triblock Surface Active Block Copolymer with Grafted Ethoxylated Fluoroalkyl Amphiphilic Side Chains for Marine Antifouling/Fouling-Release Applications. *Langmuir* **2009**, *25*, 12266−12274.
(56) Calabrese, D. R.; Wenning, B. M.; Buss, H.; Finlay, J. A.; Fischer, D.; Clare, A. S.; Segalman, R. A.; Ober, C. K. Oligopeptide-Modified Hydrophobic and Hydrophilic Polymers as Antifouling Coatings. *Green Mater.* **2017**, *5*, 31−43.
(57) Patterson, A. L.; Wenning, B.; Rizis, G.; Calabrese, D. R.; Finlay, J. A.; Franco, S. C.; Zuckermann, R. N.; Clare, A. S.; Kramer, E. J.; Ober, C. K.; Segalman, R. A. Role of Backbone Chemistry and Monomer Sequence in Amphiphilic Oligopeptide- and Oligopeptoid-Functionalized PDMS- and PEO-Based Block Copolymers for Marine Antifouling and Fouling Release Coatings. *Macromolecules* **2017**, *50*, 2656−2667.
(58) Barry, M. E.; Davidson, E. C.; Zhang, C.; Patterson, A. L.; Yu, B.; Leonardi, A. K.; Duzen, N.; Malaviya, K.; Clarke, J. L.; Finlay, J. A.; Clare, A. S.; Chen, Z.; Ober, C. K.; Segalman, R. A. The Role of Hydrogen Bonding in Peptoid-Based Marine Antifouling Coatings. *Macromolecules* **2019**, *52*, 1287−1295.
(59) Love, D. M.; Kim, K.; Goodrich, J. T.; Fairbanks, B. D.; Worrell, B. T.; Stoykovich, M. P.; Musgrave, C. B.; Bowman, C. N. Amine Induced Retardation of the Radical-Mediated Thiol-Ene Reaction via the Formation of Metastable Disulfide Radical Anions. *J. Org. Chem.* **2018**, *83*, 2912−2919.
(60) Love, D.; Fairbanks, B.; Bowman, C. Reaction Environment Effect on the Kinetics of Radical Thiol-Ene Polymerizations in the Presence of Amines and Thiolate Anions. *ACS Macro Lett.* **2020**, *9*, 174−179.
(61) Love, D. M.; Fairbanks, B. D.; Bowman, C. N. Limitations of Radical Thiol-Ene Reactions for Polymer-Polymer Conjugation. *J. Polym. Sci., Part A: Polym. Chem.* **2020**, *48*, 1699−1713.
(62) Youngblood, J. P.; Andruzzi, L.; Ober, C. K.; Hexemer, A.; Kramer, E. J.; Callow, J. A.; Finlay, J. A.; Callow, M. E. Coatings Based on Side-Chain Ether-Linked Poly(Ethylene Glycol) and Fluorocarbon Polymers for the Control of Marine Biofouling. *Biofouling* **2003**, *19*, 91−98.
(63) Krishnan, S.; Wang, N.; Ober, C. K.; Finlay, J. A.; Callow, M. E.; Callow, J. A.; Hexemer, A.; Sohn, K. E.; Kramer, E. J.; Fischer, D. A. Comparison of the Fouling Release Properties of Hydrophobic Fluorinated and Hydrophilic PEGylated Block Copolymer Surfaces: Attachment Strength of the Diatom *Navicula* and the Green Alga *Ulva*. *Biomacromolecules* **2006**, *7*, 1449−1462.
(64) Brady, R. F.; Singer, I. L. Mechanical Factors Favoring Release from Fouling Release Coatings. *Biofouling* **2000**, *15*, 73−81.
(65) Ahmed, N.; Murosaki, T.; Kakugo, A.; Kurokawa, T.; Gong, J. P.; Nogata, Y. Long-Term in Situ Observation of Barnacle Growth on Soft Substrates with Different Elasticity and Wettability. *Soft Matter* **2011**, *7*, 7281−7290.
(66) Chaudhury, M. K.; Finlay, J. A.; Chung, J. Y.; Callow, M. E.; Callow, J. A. The Influence of Elastic Modulus and Thickness on the Release of the Soft-Fouling Green Alga *Ulva linza* (Syn. *Enteromorpha linza*) from Poly(Dimethylsiloxane) (PDMS) Model Networks. *Biofouling* **2005**, *21*, 41−48.

https://doi.org/10.1021/acs.biomac.1c01474
Biomacromolecules XXXX, XXX, XXX−XXX

(67) Baek, Y.; Kang, J.; Theato, P.; Yoon, J. Measuring Hydrophilicity of RO Membranes by Contact Angles via Sessile Drop and Captive Bubble Method: A Comparative Study. *Desalination* **2012**, *303*, 23−28.
(68) Wypych, G. Table of Polymer Properties. In *Handbook of Polymers*, 2nd ed.; Wypych, G., Ed.; ChemTec Publishing, 2016.
(69) Shard, A. G. Detection Limits in XPS for More than 6000 Binary Systems Using Al and Mg Kα X-rays. *Surf. Interface Anal.* **2014**, *46*, 175−185.
(70) Wetherbee, R.; Lind, J. L.; Burke, J.; Quatrano, R. S. The First Kiss: Establishment and Control of Initial Adhesion by Raphid Diatoms. *J. Phycol.* **1998**, *34*, 9−15.
(71) Lind, J. L.; Heimann, K.; Miller, E. A.; Van Vliet, C.; Hoogenraad, N. J.; Wetherbee, R. Substratum Adhesion and Gliding in a Diatom Are Mediated by Extracellular Proteoglycans. *Planta* **1997**, *203*, 213−221.
(72) Higgins, M. J.; Molino, P.; Mulvaney, P.; Wetherbee, R. The Structure and Nanomechanical Properties of the Adhesive Mucilage That Mediates Diatom-Substratum Adhesion and Motility. *J. Phycol.* **2003**, *39*, 1181−1193.
(73) Holland, R.; Dugdale, T. M.; Wetherbee, R.; Brennan, A. B.; Finlay, J. A.; Callow, J. A.; Callow, M. E. Adhesion and Motility of Fouling Diatoms on a Silicone Elastomer. *Biofouling* **2004**, *20*, 323−329.
(74) Heydt, M.; Pettitt, M. E.; Cao, X.; Callow, M. E.; Callow, J. A.; Grunze, M.; Rosenhahn, A. Settlement Behavior of Zoospores of *Ulva linza* during Surface Selection Studied by Digital Holographic Microscopy. *Biointerphases* **2012**, *7*, No. 33.
(75) Fletcher, R. L.; Callow, M. E. The Settlement, Attachment and Establishment of Marine Algal Spores. *Br. Phycol. J.* **1992**, *27*, 303−329.
(76) Callow, J. A.; Callow, M. E. The Ulva Spore Adhesive System. *Biological Adhesives*; Springer: Berlin, Heidelberg, 2006; Vol. 3, pp 63−78.
(77) Callow, J. A.; Callow, M. E.; Ista, L. K.; Lopez, G.; Chaudhury, M. K. The Influence of Surface Energy on the Wetting Behaviour of the Spore Adhesive of the Marine Alga *Ulva linza* (Synonym *Enteromorpha linza*). *J. R. Soc. Interface* **2005**, *2*, 319−325.
(78) Ederth, T.; Nygren, P.; Pettitt, M. E.; Ostblom, M.; Du, C. X.; Broo, K.; Callow, M. E.; Callow, J.; Liedberg, B. Anomalous Settlement Behavior of *Ulva linza* Zoospores on Cationic Oligopeptide Surfaces. *Biofouling* **2008**, *24*, 303−312.
(79) Ederth, T.; Pettitt, M. E.; Nygren, P.; Du, C.-X.; Ekblad, T.; Zhou, Y.; Falk, M.; Callow, M. E.; Callow, J. A.; Liedberg, B. Interactions of Zoospores of *Ulva linza* with Arginine-Rich Oligopeptide Monolayers. *Langmuir* **2009**, *25*, 9375−9383.
(80) Rosenhahn, A.; Finlay, J. A.; Pettit, M. E.; Ward, A.; Wirges, W.; Gerhard, R.; Callow, M. E.; Grunze, M.; Callow, J. A. Zeta Potential of Motile Spores of the Green Alga *Ulva linza* and the Influence of Electrostatic Interactions on Spore Settlement and Adhesion Strength. *Biointerphases* **2009**, *4*, 7−11.
(81) Sullivan, T.; Regan, F. Marine Diatom Settlement on Microtextured Materials in Static Field Trials. *J. Mater. Sci.* **2017**, *52*, 5846−5856.
(82) Sweat, L. H.; Johnson, K. B. The Effects of Fine-Scale Substratum Roughness on Diatom Community Structure in Estuarine Biofilms. *Biofouling* **2013**, *29*, 879−890.
(83) Granhag, L. M.; Finlay, J. A.; Jonsson, P. R.; Callow, J. A.; Callow, M. E. Roughness-Dependent Removal of Settled Spores of the Green Alga *Ulva* (Syn. *Enteromorpha*) Exposed to Hydrodynamic Forces from a Water Jet. *Biofouling* **2004**, *20*, 117−122.
(84) Schumacher, J. F.; Carman, M. L.; Estes, T. G.; Feinberg, A. W.; Wilson, L. H.; Callow, M. E.; Callow, J. A.; Finlay, J. A.; Brennan, A. B. Engineered Antifouling Microtopographies - Effect of Feature Size, Geometry, and Roughness on Settlement of Zoospores of the Green Alga *Ulva*. *Biofouling* **2007**, *23*, 55−62.
(85) Vucko, M.; Pooleb, A. J.; Carla, C.; Sextonc, B. A.; Glennc, F. L.; Whaland, S.; Nysa, R.-D. Using Textured PDMS to Prevent Settlement and Enhance Release of Marine Fouling Organisms. *Biofouling* **2014**, *30*, 1−16.
(86) Leonardi, A.; Zhang, A. C.; Düzen, N.; Aldred, A.; Finlay, J. A.; Clarke, J. L.; Clare, A. S.; Segalman, R. A.; Ober, C. K. Amphiphilic Nitroxide-Bearing Siloxane-Based Block Copolymer Coatings for Enhanced Marine Fouling Release. *ACS Appl. Mater. Interfaces* **2021**, *13*, 28790−28801.
(87) Granhag, L. M.; Finlay, J. A.; Jonsson, P. R.; Callow, J. A.; Callow, M. E. Roughness-Dependent Removal of Settled Spores of the Green Alga *Ulva* (syn. *Enteromorpha*) Exposed to Hydrodynamic Forces from a Water Jet. *Biofouling* **2004**, *20*, 117−122.
(88) Schönemann, E.; Koc, J.; Karthäuser, J. F.; Özcan, O.; Schanzenbach, D.; Schardt, L.; Rosenhahn, A.; Laschewsky, A. Sulfobetaine Methacrylate Polymers of Unconventional Polyzwitterion Architecture and Their Antifouling Properties. *Biomacromolecules* **2021**, *22*, 1494−1508.
(89) Heuberger, M.; Drobek, T.; Vörös, J. About the Role of Water in Surface-Grafted Poly(Ethylene Glycol) Layers. *Langmuir* **2004**, *20*, 9445−9448.
(90) Zheng, J.; Li, L.; Tsao, H. K.; Sheng, Y. J.; Chen, S.; Jiang, S. Strong Repulsive Forces between Protein and Oligo (Ethylene Glycol) Self-Assembled Monolayers: A Molecular Simulation Study. *Biophys. J.* **2005**, *89*, 158−166.

https://doi.org/10.1021/acs.biomac.1c01474
Biomacromolecules XXXX, XXX, XXX−XXX